Simulation of a Space-Based Microlensing Survey for Terrestrial Extra-Solar Planets

David P. Bennett & Sun Hong Rhie

Department of Physics, University of Notre Dame, Notre Dame, IN 46556

email: bennett@nd.edu, srhie@nd.edu

ABSTRACT

We show that a space-based gravitational microlensing survey for terrestrial extra-solar planets is feasible in the near future, and could provide a nearly complete picture of the properties of planetary systems in our Galaxy. We present simulations of such a survey using a $1-2$m aperture space telescope with a ~ 2 square degree field-of-view which is used to continuously monitor $\sim 10^8$ Galactic bulge main sequence stars. The microlensing techniques allows the discovery of low mass planets with high signal-to-noise, and the space mission that we have studied are sensitive to planets with masses as low as that of Mars. By targeting main sequence source stars, which can only be resolved from space, the space-based microlensing survey is able to detect enough light from the lens stars to determine the spectral type of one third of the lens stars with detected planets, including virtually all of the F, G, and K stars which comprise one quarter of the event sample. This enables the determination of the planetary masses and separations in physical units, as well as the abundance of planets as a function of stellar type and distance from the Galactic center. We show that a space-based microlensing planet search program has its highest sensitivity to planets at orbital separations of 0.7-10 AU, but it will also have significant sensitivity at larger separations and will be able to detect free-floating planets in significant numbers. This complements the planned terrestrial planet transit missions which are sensitive to terrestrial planets at separations of ≤ 1 AU. Such a mission should also detect $\sim 50,000$ giant planets via transits, and it is, therefore, the only proposed planet detection method that is sensitive to planets at all orbital radii.

Subject headings: dark matter - gravitational lensing

1. Introduction

The discovery of the first extra-solar planets a few years ago (Mayor & Queloz 1995; Marcy & Butler 1996; Butler & Marcy 1996) has spurred the growth of a new branch of observational astronomy, the study of extra-solar planets. The success of the precision radial velocity technique has been spectacular (Marcy, Cochran & Mayor 2000; Perryman 2000; Marcy & Butler 2000) with the discovery of more than 70 extra-solar giant planets in the past seven years. This technique is sensitive enough to detect Jupiter-mass planets in Jupiter-like orbits, and it is anticipated that such planets will be discovered in the next few years as the duration of the radial velocity monitoring programs approaches Jupiter's orbital period of 12 years. The dramatic success of these radial velocity extra-solar planet search programs has encouraged the astronomical community to address the far more ambitious goal of searching for Earth-like extra-solar planets (Dressler et al. 1996) because such planets seem best suited for life. The search for Earth-like extra-solar planets has now become a major NASA goal. It is likely that it will require the development of new extra-solar planet search techniques since it is thought that the intrinsic radial velocity noise of stars will limit this technique to planets with masses $\gtrsim$ a few $\times 10^{-4}$ of the host star's mass which is 100 times greater than an Earth mass.

A number of extra-solar planet search methods have been proposed that should be able to detect planets in the Earth mass range (Perryman 2000). The Space Interferometry Mission (SIM) (Danner & Unwin 1999) will be able to detect planets of a few Earth masses around nearby stars via their astrometric effects on the stars they orbit. But, SIM requires some technical development before it will be ready to fly, and it is not required to have the capability to detect Earth mass planets. The most ambitious planet search missions being considered are the Terrestrial Planet Finder (TPF) (Beichman 1998) and Darwin (Fridlund 2000) missions which will have the ability to directly detect Earth-like planets around nearby stars. However, these missions require a considerable amount of technological development before they will be ready to fly. Also, the McKee-Taylor Decadal Survey Committee (McKee & Taylor 2000) qualified its endorsement of the TPF mission with the condition that the abundance of Earth-size planets be determined prior to the start of the TPF mission.

The gravitational microlensing and transit techniques are two methods that have sensitivity to terrestrial planets, but are technically easier than SIM or TPF. These missions are sensitive to planets orbiting distant stars, so they are most useful for obtaining statistical information regarding the abundance of planetary systems. The transit technique is employed by the COROT mission (Schneider et al. 1998) which is slated for launch by CNES in 2004, the the Eddington mission (Deeg et al. 2000) which has been selected as an ESA F2/F3 "reserve" mission, and Kepler mission (Koch et al. 1998) which is under development for NASA's Discovery Program. However, these surveys share the property that the transit signal due to an Earth-like planet is a photometric variation of only $\sim 0.01\,\%$. This is only a few times above the anticipated photometric noise, so these mission generally require the observation of 3 or 4 transits in order to avoid false detections due to photometric noise. Even then, one false detection is expected over the course of the mission (Koch et al. 2000). The requirement for 3-4 transits limits the sensitivity of the transit technique to planets with orbital periods of $\lesssim 1$ year due to the limited mission duration and low transit probability for planets in longer period orbits. In contrast, the sensitivity of a space-based microlensing planet search program extends from about $0.7\,$AU to infinity, with significant sensitivity to free-floating planets. Thus, the combination of a transit survey like Kepler with a space-based microlensing planet search will determine the abundance of terrestrial and larger planets at all orbital radii.

Knowledge of the general properties of planetary systems is important even if we are primarily interested in habitable planets because the issue of planetary habitability is a complex and poorly defined one. The Earth's habitability is a consequence of a complex interplay of physical processes (Lunine 1999) that are not likely to be replicated in exactly the same way on other worlds. While the fundamental requirement is assumed to be stable liquid water over geologic time, many diverse factors come into play in establishing habitable ecosystems (Des Marais et al. 2001). More importantly, we do not know what the outcome of a different combination or timing of such processes would be in terms of habitability (Chyba et al. 2000). A non-exhaustive list of the potential requirements for habitability include the presence of giant planets in 5-10 AU orbits (Lunine 2001), the presence of a large moon to stabilize the planetary spin axis (Ward 1982), main sequence stellar type of F, G, or K (Ward and Brownlee 2000; Kasting 1997). Also, the traditional notion that a narrow range of semi-major axes are consistent with the presence of liquid water (Kasting, Whitmire & Reynolds 1993) is challenged by the evidence for liquid water on the early Mars (Carr 1996). The length and incompleteness of this shopping list demands survey missions be initiated soon to map out the geometries of extra-solar planetary systems prior to much more expensive missions whose intent is to spectroscopically examine extra-solar terrestrial planets. With its high sensitivity to low-mass planets at a wide range of separations, a space-based gravitational microlensing survey would be the ideal mission for a comprehensive survey of the properties of planetary systems.

1.1. The Gravitational Microlensing Technique

The gravitational microlensing technique (Mao & Paczynski 1991; Gould & Loeb 1992; Bennett et al. 2000), has the unique property that the strength of the planet's photometric microlensing signal is nearly independent of the planetary mass. Instead of a weaker signal, the microlensing signals of low-mass planets have a shorter duration and a lower detection probability than those of high-mass planets. (This argument breaks down for planetary masses below $0.1\mathrm{M}_\oplus$ because such planets lens only a fraction of the main sequence source star disks.) This means that a microlensing survey with frequent observations of a very large number of stars will be able to detect terrestrial planets at high signal-to-noise (Tytler 1996; Bennett & Rhie 1996; Wambsganss 1997; Bennett & Rhie 2000). The microlensing technique employs stars in the Galactic bulge which act as sources of light rays which are bent by the gravitational fields of stars in the foreground: on the near side of the Galactic bulge, or in the disk. Planets which may orbit these "lens" stars can be detected when the light rays from one of the lensed images pass close to a planet orbiting the lens star. The gravitational field of the planet distorts this lensed image causing a significant variation of the gravitational microlensing light curve from the standard single lens light curve. This planetary deviation is typically of order $\sim 10\%$, and it has a duration of a few hours to a day compared to the typical 1-2 month duration for lensing events due to stars.

The main challenge for a microlensing planet search project is that microlensing events are rare. Only about 3×10^{-6} of Galactic bulge stars are microlensed at any given time (Udalski et al. 1994; Alcock et al. 1997; Alcock et al. 2000b), and only $\sim$ 2% of earth-mass planets orbiting these stars will be in the right position to be detected (Bennett & Rhie 1996). The sensitivity limit of the gravitational microlensing technique is set by the finite angular size of the source stars because a very low mass planet will only deflect the light rays from a fraction of the source star's disk. This can wash out the photometric signal of the planet. For main sequence source stars in the Galactic bulge, the sensitivity limit is about $0.1\mathrm{M}_\oplus$, but for giant source stars, it is $> 1\mathrm{M}_\oplus$. Thus, a gravitational microlensing search for terrestrial planets must use main sequence source stars. However, the density of bright main sequence stars in the central Galactic bulge is several stars per square arc second, so angular resolution of $\ll 1$ arc sec is necessary to resolve these stars.

In order to accurately characterize the parameters of the planets discovered via microlensing (Gaudi & Gould 1997; Gaudi 1998), we must have photometry of $\sim$ 1% accuracy sampled several times per hour over a period of several days (*i.e.* a factor of a few longer than the planetary light curve deviation). The microlensing event light curves must also be sampled continuously for periods of more than 24 hours, in order to unambiguously characterize the planetary signals in microlensing light curves. This allows both the full planetary deviation as well as the periods before and after it to be observed.

1.2. Ground-based Microlensing Planet Searches

The earliest discussions of detecting terrestrial planets via gravitational microlensing generally considered it to be a technique for ground-based observations (Tytler 1996; Bennett & Rhie 1996; Wambsganss 1997). However, these early estimates proved to be overly optimistic in a number of respects. Peale (1997) performed a simulation of what sort of planets could be detected by a global network of $\sim 2\,$m telescopes as suggested by (Tytler 1996) showed that a substantial number of possible planet detections would be missed due to poor weather and geographic limitations on the locations of ground based telescopes, but his results are over-optimistic for several different reasons. For example, no account was taken of variations in atmospheric seeing or of the poorer average seeing from the non-Chilean observing sites. Sackett (1997) sought to avoid the problems of the poorer observing sites by proposing a search employing only a single, excellent observing site, Paranal under the assumption that the planetary signals of terrestrial planets would be brief enough that some could be fully characterized by observations spanning $\lesssim 8\,$hours.

All of these papers considered the monitoring Galactic bulge turn-off stars. Ground-based color magnitude diagrams of the dense Galactic bulge fields observed by the microlensing surveys seemed to show that there were very large numbers of these stars. Turn-off stars are stars that have recently exhausted the Hydrogen fuel in their cores, and are just beginning the Hydrogen shell burning phase. They are 1-2 magnitudes brighter than the stars at the top of the main sequence, but have similar colors. Their radii are small enough to allow the detection of Earth-mass planets via microlensing. However, this is a relatively brief phase of stellar evolution, and so their apparent abundance in Galactic bulge seemed odd. In fact, this abundance was not confirmed with HST data (Holtzman et al. 1998). The apparent abundance of these "turn-off" stars is an artifact the stellar crowding in these central Galactic bulge fields; the density of main sequence stars is too high for them to be individually resolved, and several main sequence stars blended together are typically identified as a single "turn-off" star. This is illustrated in Fig. 1 which compares two ground based images of microlensing event MACHO-96-BLG-5 to an HST image and a simulated image from a proposed space-based microlensing planet search telescope. Clearly, density of bright main sequence stars (like the one indicated) is too high for these stars be individually resolved from the ground. This stellar blending phenomena has been widely discussed in the gravitational microlensing literature (di Stefano & Esin 1995; Wozniak & Paczynski 1997; Han 1997), and there is now strong evidence that virtually all of the microlensing events involving apparent bulge "turn-off" source stars are, in fact, blended microlensing events with main sequence source stars (Alcock et al. 2000a; Alcock et al. 2000b). This blending of source stars makes microlensing planet searches much more difficult because the planetary signal will be confined to the flux from only one of the blended stars, but all of the blended stars will contribute to the photometric noise.

One can hope to compensate for the increased photometric noise caused by blended by moving to relatively large wide field-of-view ground-based telescopes, such as the $4\,$m VISTA telescope or the $\sim 8\,$m LSST (the Large Synoptic Survey Telescope - recommended by the McKee-Taylor Committee (McKee & Taylor 2000)). A detailed study of such potential observing programs reveals that a survey from an excellent observing site such as Paranal is about two orders of magnitude less sensitive than a space-based microlensing planet search program (Bennett & Rhie 2002). A critical problem for such a ground-based program is that the typical duration of a microlensing light curve deviation due to an Earth-mass planet is nearly 24 hours. This is about an order of magnitude longer than the Einstein radius crossing time, which was used as the characteristic planetary event duration in a previous study which advocated a microlensing planet survey from a single site (Sackett 1997). With a realistic distribution of event durations, however, we find that only a very small subset of Earth-mass planetary microlensing signals can be detected and characterized. The detectable Earth-mass planet events from such a survey also suffer from several undesirable selection effects. There is a much higher fraction of high magnification events with planetary separations very close to the Einstein radius, and these events provide essentially no information on the abundance of planets as a function of orbital separation. Finally, few of the events which are detected with these ground based surveys allow the detection of the lens star, so the planetary abundance as a function of spectral type also cannot be measured from the ground.

1.3. Microlensing Planet Search Space Mission Requirements

The primary intent of this paper is to investigate low cost space missions which employ the gravitational microlensing technique to detect terrestrial planets orbiting other stars. The basic requirements for such a mission are that $\sim 10^8$ Galactic bulge main sequence stars must be observed almost continuously at intervals of 20 minutes, or less for periods of at least several months. Photometric accuracy of $\sim 1\,\%$ or better is needed, and this implies that the angular resolution of the images must be < 0.4" in order to resolve main sequence stars in the crowded central Galactic bulge fields. The required frequent photometric measurements of such a large number of stars requires relatively high data rate of $\gtrsim 10\,$Mbits/sec depending upon the data compression scheme that is used.

While the wide-field imaging capabilities required for such a mission substantially exceed the capabilities of existing space telescopes, it it can be undertaken at a relatively modest cost, within the limits of NASA's MIDEX or Discovery programs. There may also be an opportunity to combine a microlensing planet search mission with another major science program, such as a deep, wide field, weak gravitational lensing survey or a high-redshift Supernova search similar to the proposed SuperNova Acceleration Probe[1] (SNAP). It might also be possible to combine a microlensing planet search mission with an asteroseismology program such as the Eddington mission[2] mission if such a mission were designed with good in-focus optics.

Two proposals for microlensing planet search missions have been submitted to NASA in 2001. The Galactic Exoplanet Survey Telescope (GEST[3]) was submitted to NASA's MIDEX Program, and the Survey for Terrestrial ExoPlanets (STEP) was submitted to NASA's Extra Solar Planets: Advanced Concepts program. We will use the GEST MIDEX proposal as the baseline for our discussions of planet detection sensitivity, but we will also investigate the variation of the planet detection sensitivity on the parameters of the mission.

The terrestrial planetary signals in gravitational microlensing light curves that these missions would study show significant variations on time scales ranging from 20-30 minutes to about a day. Therefore, it is important that a microlensing planet search telescope be in an orbit which allows continuous viewing of the Galactic bulge. The orbit proposed for GEST is a polar orbit with an altitude of $\sim 1200\,$km oriented to keep the Galactic bulge in the continuous viewing zone, while the STEP mission would employ a nearly circular geosynchronous orbit inclined by 28.7° (the latitude of Cape Canaveral) from the equator and by $\sim 50^\circ$ with respect to the ecliptic plane. Even higher Earth orbits, such as the 14-day "Prometheus" orbit proposed for SNAP, would also be acceptable, but Earth-trailing orbit might make it difficult to achieve the required data rate.

The GEST and STEP designs call for 1.0m and 1.5m aperture telescopes each with a 2.2 square de-

[1] See `http://snap.lbl.gov` for information regarding the proposed SNAP mission

[2] See `http://astro.esa.int/SA-general/Projects/Eddington/` for information on ESA's Eddington mission.

[3] More information on the Galactic Exoplanet Survey Telescope is available at `http://bustard.phys.nd.edu/GEST/`

gree field of view and a three mirror anastigmat design. The field of view is elliptical with an axis ratio of about 2:1, and the GEST proposal would use an array of 32 3072×6144 pixel Lincoln Labs high resistivity CCDs for enhanced sensitivity in the near IR. The STEP proposal would use a combination of these same Lincoln Labs CCDs and Rockwell HgCdTe IR detector arrays. These IR detectors would be similar to a design intended for the Hubble Space Telescope's Wide Field Camera 3 with a long wavelength cut-off of $\sim 1.7\,\mu$ to allow radiative cooling from a high Earth orbit. The quantum efficiency of these detectors is displayed in Fig. 2 along with the reddened spectrum of a typical bulge source star. The standard CCD curve is typical of most broadband astronomical CCD detectors (such as those manufactured by Marconi, SITe, or Fairchild). Both the Lincoln Labs and LBL devices use high resistivity Silicon to enhance sensitivity in the near IR, and the LBL devices have higher sensitivity near $\lambda = 1.0\mu$ because they are more opaque at this wavelength due to their 300μ thickness vs. 50μ for the Lincoln devices.

The overall sensitivity of the detectors is given by the integral of the product of the source spectrum, the QE curve, and an additional function describing the throughput of the rest of the optical system. If we assume that the optical system has no other significant wavelength dependence besides the detectors, then we find sensitivity improvements of 44%, 62%, and 150% for the Lincoln, LBL, and Rockwell detectors, respectively when compared to the sensitivity of the standard astronomical CCD. At the time of this writing, only the standard and Lincoln CCDs can be produced in the large quantities needed for a microlensing planet search mission, but this situation may change in the near future.

It is anticipated that GEST and STEP will take ~ 100 second exposures at 2 minute intervals which would be co-added into ten minutes exposures. Assuming digitization at 14 bits/pixel, this gives a total data rate of $14\,$Mbits/sec if no data compression is employed.

In order to make use of the high angular resolution available from space, it is necessary for the space-based telescope to have high pointing stability. We require that the pointing be stable to 10% or better of the assumed 0.2 arc second CCD pixel size. This should be achievable with three-axis stabilized, ultra-low jitter spacecraft, such as Lockheed's LM-900, as long as a fine-guidance signal is provided from guide CCDs in the focal science focal plane which would be read out a few times a second. Another option, which could correct higher frequency pointing jitter, would be to use a fast-guiding secondary mirror. The only pointing variation needed during the ~ 8 month Galactic bulge season would be a sub-pixel scale dither pattern needed to ensure that the photometric accuracy remains very close to the photon noise limit (Lauer 1999; Gilliland et al. 2000).

In this paper, we present the results of a detailed simulation of a space-based microlensing planet search mission. In section 2, we explain the assumptions and the details of our simulation and argue that our assumptions are conservative. In section 3, we present the details of our results including example light curves, the predicted planet detection sensitivity to bound and free-floating planets, and the prospects for direct observations of the lens stars. There is also a brief discussion of the $\sim 50,000$ planets that such a mission is likely to detect via transits. Finally, in section 4, we summarize the scientific results to be expected from a space-based microlensing planet search mission.

2. Mission Simulation Details

In order to simulate a space-based microlensing planet search mission, we must make assumptions regarding the source stars, the lens star systems and the telescope. Our distribution of source stars is based upon the Galactic bulge luminosity function of Holtzman et al. (1998). Following the GEST proposal, we select a field at Galactic coordinates $l \approx 1.2^\circ$, $b \approx -2.4^\circ$, which is closer to the Galactic Center than the Baade's window field observed by Holtzman et al. This implies that both the star density and the reddening will be higher, and we split the field into two pieces for the purposes or our simulations in order to account for the gradient of the star density with Galactic latitude. The two half-fields have central Galactic latitudes of $b = -2.0°$ and $-2.8°$, and we have assigned them star densities of 2.06 and 1.55 times the Holtzman et al. (1998) star density measured at $b = -3.9°$ based upon number counts of "red clump" stars in the MACHO fields (Popowski et al. 2000). The I-band extinctions for these two half fields are assumed to be $A_I = 1.6$ for the inner half field and $A_I = 1.5$ for the outer half field. These reddening values can be obtained from the Schlegel, Finkbeiner & Davis (1998) dust map with a correction for stellar emission as advocated by Stanek (1999) or by assuming that the excess IR emission is proportional to the "red clump" star number counts.

Another very crucial physical input for our simulation is the microlensing probability (or optical depth, τ) towards the Galactic bulge. Measured values are $\tau = 3.3 \pm 1.2 \times 10^{-6}$ at $l = 0.9°$, $b = -3.8°$ (Udalski et al. 1994), $\tau = 3.9^{+1.8}_{-1.2} \times 10^{-6}$ at $l = 2.55°$ and $b = -3.64°$ (Alcock et al. 1997), and $\tau = 3.23^{+0.52}_{0.50} \times 10^{-6}$ at $l = 2.68°$ and $b = -3.35°$ (Alcock et al. 2000b). We have used this latest measurement because it is based upon the largest sample, and it is closest to the theoretical estimates. Theoretical determinations of the scaling of the microlensing probability with position (Bissantz et al. 1997; Peale 1998) indicate that the microlensing probability at GEST's outer half field ($l = 1.2°$, $b = -2.8°$) should be 1.2-1.3 times larger than at $l = 2.68°$, $b = -3.35°$, while the increase at the inner half field ($l = 1.2°$, $b = -2.0°$) should be a factor 1.4-1.8. For the purposes of this simulation, we have selected a conservative choice for the microlensing probability, $\tau = 2.43 \times 10^{-6}$ at $l = 2.68°$ and $b = -3.35°$ which we then scale to $\tau = 2.9 \times 10^{-6}$ at $l = 1.2°$, $b = -2.8°$, and $\tau = 3.9 \times 10^{-6}$ at $l = 1.2°$, $b = -2.0°$. This is the 1.6σ lower limit on the value of τ extrapolated to our selected field.

The mass function of the lens stars is assumed to follow the a conventional power law form, $f(m) \propto m^{-\alpha}$ where $f(m)dm$ is the number of stars in the mass interval m to $m + dm$. We use a mass function similar to those advocated by Zoccali et al. (2000) and Kroupa (2000) which imply different values of α in different mass intervals: $\alpha = 2.3$ for $m > 0.8\mathrm{M}_\odot$, $\alpha = 1.33$ for $0.15\mathrm{M}_\odot < \mathrm{m} < 0.8\mathrm{M}_\odot$, and $\alpha = 0.3$, for $0.05\mathrm{M}_\odot < \mathrm{m} < 0.15\mathrm{M}_\odot$. The mass function is truncated at $0.05\mathrm{M}_\odot$ in order to keep the distribution of microlensing event timescales consistent with the observations of Alcock et al. (2000b). Stellar remnants are also included with white dwarfs contributing 13% of the lens stars, while neutron stars and black holes contribute < 1% and < 0.1% of the lens stars, respectively.

With these parameters for the properties of the inner Galaxy, we precede to run our simulations as follows:

1. We create an artificial image with stars $0 \leq M_I \leq 9$ at random locations in an artificial image using a "pseudo-gaussian" profile (as in DOPHOT (Schechter, Mateo & Saha 1993)) with a FWHM of 0.24." Brighter stars are not included, but we assume that 5% of the 2.1 square degree field of view is lost due to bright, saturated stars or CCD defects.

2. A stellar lensing event is selected for each star in the frame with lens parameters selected at random assuming the mass function described above and a density and velocity distribution from a standard model of the Galaxy (Han & Gould 1997). All stellar lensing events are assumed to have an impact parameter of ≤ 3 Einstein radii, and the source stars are assumed to reside at $0.5\,$kpc behind the Galactic Center which is at $R_0 = 8\,$kpc.

3. The orientation of each "exo-ecliptic" plane is selected at random, and then planet locations are selected by assigning each planet a random orbital phase within this plane. The planets are assumed to follow circular orbits with radii between 0.25 and 30 AU and mass fractions ranging from $\epsilon = 3 \times 10^{-7}$ to $\epsilon = 10^{-3}$.

4. Planetary lensing light curves are constructed assuming measurements every ten minutes. Finite source effects are incorporated assuming

a mass radius relationship taken from Bertelli et al. (1994).

5. The CCD camera is assumed to detect 13 photons per second from an $I = 22$ star. This can be achieved with a 1.5m telescope with standard CCDs employing a 650-900nm passband, or with a 1.0m telescope with high-resistivity Lincoln labs or LBL CCDs with a 500-1000nm passband.

6. Light curve error bars are generated under the assumption that the photometric accuracy is limited by photon statistics for noise levels down to 0.3%. This level of accuracy has been demonstrated with highly undersampled HST images of very crowded star fields (Lauer 1999; Gilliland et al. 2000). The key to this photometric accuracy is to recover the diffraction limited resolution with a sub-pixel scale dither pattern. The undersampling of these HST images is similar to the level of undersampling for the proposed GEST mission, as shown in Fig. 1. In addition to the source star, the lens star and nearby stars with images that are blended with the source star are assumed to contribute to the photon noise.

7. A single lens, point source light curve is fit to each event, and planet detections are signaled by an excess fit χ^2. We measure the planetary signal with the $\Delta\chi^2$ which is the difference between the χ^2 for the single lens fit and the correct planetary lensing fit. Our detection threshold is $\Delta\chi^2 \geq 160$ which is the equivalent of a 12.5σ detection.

One potential drawback with our method for identifying planet detections is that planet detections may be incorrectly indicated for events with very high magnification because the effects of the finite angular size of the source star may be seen. These high magnification events also have higher sensitivity to planets than lower magnification events (Griest & Safizadeh 1998) because the source star must necessarily pass close to the "stellar" caustic curve which will be distorted due to the presence of planets. However, the determination of the planetary mass fraction (ϵ) and separation can be difficult for events detected due to the stellar caustic (Dominik 1999). Thus, it is not yet clear how useful such detections will be, although they do present enhanced sensitivity to multiple planets (Gaudi, Naber & Sackett 1998). Because of this uncertainty, we have excluded planets detected in events with maximum magnifications > 200.

3. Expected Results

3.1. Planetary Parameters from Microlensing

The diversity of microlensing planetary light curves has been studied quite extensively (Mao & Paczynski 1991; Gould & Loeb 1992; Bolatto & Falco 1994; Bennett & Rhie 1996; Wambsganss 1997; Gaudi & Gould 1997; Gaudi 1998), and these studies have shown that it is possible to measure both the planetary mass fraction, ϵ, and the planet-star separation from the light curve shape. The duration of the planetary light curve deviation gives ϵ. The overall magnification of the light curve at the time of the planetary deviation and the basic shape of the planetary deviation give the separation. However, the transverse separation, a, is only determined in units of the Einstein ring radius,

$$R_E = 2.85\,\mathrm{AU}\sqrt{\frac{M}{\mathrm{M}_\odot}\frac{D}{1\,\mathrm{kpc}}}\,, \tag{1}$$

which is just the radius of ring image for a single lens of mass M that is perfectly aligned with the source star. $D = D_l(D_s - D_l)/D_l$, where D_l and D_s are the distances to the lens and source stars, respectively.

For a source star in the Galactic bulge, R_E is typically $\sim 2\,\mathrm{AU}$, and it ranges from 1-4 AU, so a measurement of a/R_E will yield an estimate of a that is good to a factor of 2. For most of the terrestrial planet detections, however, we can do somewhat better than this because we can also measure the time for the lens center-of-mass to cross the source star radius, t_s. This parameter is measurable for events in which the source comes very close to or crosses one of the lens caustics. This occurs for a large fraction of the terrestrial planet events, but there are many of the giant planet lensing events that are detectable without a close approach to a caustic. Precise values of a and M can be obtained for events in which the lens can be detected either via multi-color photometry, spectroscopy, or proper motion, as the lens separates from the source in the years after the event. This should be possible for about one third of the events including virtually all of the F, G and K star lenses. (See subsection 3.7 for a more detailed discussion of source star identification.)

3.2. Event Light Curves

Examples of the planetary light curves from our GEST mission simulation are shown in Figures 3-5. The data are shown with the error bars determined as described above, and the light curves are presented with the sampling interval of 10 minutes that was used for the event detection calculations. While the error bars are meant to indicate the $1\,\sigma$ uncertainties, we have not added this noise to the data points shown in Figures 3 and 4 because of the high density of data points in these figures. These light curves are meant to illustrate the range of planetary light curves that a space-based microlensing survey should detect. They also represent the range of signal-to-noise of the terrestrial planet detections in our GEST simulations. Figure 3(a) represents one of the highest signal-to-noise planet detections with the Earth:Sun mass ratio of $\epsilon = 3 \times 10^{-6}$, and Figure 3(b) is an event which barely passes our event detection cut of $\Delta\chi^2 \geq 160$. The other events have more typical signal-to-noise.

We've assumed that the photometric accuracy of a space-based microlensing survey will be dominated by photon statistics and that systematic errors will not become dominant until the statistical errors reach $< 0.3\%$ (in 5 co-added $100\,$sec exposures). However, Figures 3 and 4 illustrate that most of the planet detections are made with lower precision photometry, with photometric errors of $\sim 1\%$ dominated by photon statistics.

These events serve to illustrate why ground based microlensing searches are not effective for the detection of terrestrial planets (Bennett & Rhie 2000; Rhie et al. 2000b). The necessity of using main sequence target stars for a microlensing program to find terrestrial planets means that the accuracy of photometry is compromised by the blending of the source star images as demonstrated in Fig. 1. This is true even if the planet search program is limit to the best ground based observing sites such as Paranal (Sackett 1999). This blending with neighboring stars less than an arc second away substantially reduces the photometric signal-to-noise and would make the events shown in Figs. 3(b)-(d) undetectable. The event shown in Fig. 3(a) would have a large enough signal to be detectable from a ground-based program, but since the planetary deviation lasts for more than 24 hours, it would be poorly sampled from a single site. Follow-up observations from sites at other longitudes would be of little help because the poorer seeing at these sites would make the photometry too noisy to be very useful in characterizing the properties of the detected planet.

3.2.1. Light Curves for Multiple Planets and Moons

Figure 4 shows events in which multiple planets are detected. Most multiple planet events have light curves that are very similar to single planet events except that that are two different planetary deviation regions. We've run simulations of "solar-type" planetary systems in which every stellar lens is assumed to have planets with the same mass fractions as the planets in the solar system and with the same separations. Most of the multiple planet detections in our simulations are similar to Figure 4(a) in which both the "Jupiter" and "Saturn" planets are detected. In about 25% of the cases where the "Saturn" planet is detected, the Jupiter planet is also detected. This is a consequence of the fact that Saturn's orbital semi-major axis is only a factor of 1.8 larger than Jupiter's orbital semi-major axis. Such orbits are stable only if they are close to circular, so a space-based microlensing survey will be able to provide information on the abundance of giant planets with nearly circular orbits by measuring the frequency of double planet detections and the ratios of their separations. This is important information as giant planets in Jupiter or Saturn-like orbits are thought to be required for the delivery of volatiles, such as water, to the inner planets in the habitable zone (Lunine 2001).

Events in which a terrestrial planet and a "Jupiter" are detected, such as the event shown in Figure 4(b) are more rare. In part, this is because the lower mass of the terrestrial planet means that less of them will be detected, but another factor of is that the ratio of Jupiter's semi-major axis to that of the terrestrial planets is a factor of 3.5-7 rather than the factor of 1.8 ratio between the Jupiter and Saturn orbital distances. Because of this, only 10-15% of the detected terrestrial planets will also have a Jupiter detection.

The detection sensitivity for multiple planets depends more on the telescope size and the assumed level of systematic photometry errors than the sensitivity for single planets does. More sensitive photometry increases the probability that a planet can be detected in the light curve of a microlensing event, and the number of double planets detected depends on this probability squared.

In order to estimate the sensitivity for detecting multiple planets, we have calculated the detection probabilities for lenses with planetary systems with the same planetary mass fractions and separations as the planets of our own Solar System. For the parameters of the proposed GEST mission, we find that a total of about $150f$ multiple planet systems will be discovered, where f is the fraction of planetary systems that resemble our own. About $13f$ of these will be terrestrial-giant planet pairs, and the remainder will be multiple planet detections consisting of only giant planets. (These numbers assume that a lower detection threshold of 9σ can be used for the second planets to be detected because there is a much smaller number of light curves that must be searched for multiple planets.) A substantial improvement in sensitivity can be obtained with the parameters of the STEP mission: a 1.5m telescope with a 2.2 square degree field-of-view. Half of the focal plane would use Lincoln Labs near-IR optimized CCD detectors and the other half would use the HgCdTe IR arrays with a 1.7μm cutoff. If we assume that the photometry is limited by systematic errors of 0.15% in a 10 minute exposure, then our simulation indicate a total of $490f$ multiple planet detections with $45f$ of these being terrestrial-giant planet pairs.

It is also possible to detect the large moons of terrestrial planets as shown in Fig. 5. The semi-major axis of the moon's orbit is about 0.8 times the Earth's Einstein radius, so systems like our own should be detectable. Because the planet-moon separation is likely to be similar to the planetary Einstein radius, the light curve deviations due to the planet and moon are likely to be closely spaced in time or even overlapping as in the example shown in Fig. 5(b). Nevertheless, most of the light curve deviations due to planet+moon systems are well approximated by the sum of the deviations due the two minor masses by themselves. A more systematic study of the detection of planet plus moon systems by microlensing will be carried out in a future paper.

3.3. Planet Detection Sensitivity

The major goal of our simulations is to determine the sensitivity of a space-based microlensing survey. The sensitivity to planets orbiting each of the lens stars depends on a large number of factors including the event timescale, the size of the photometric error bars, and the angular size of the source star. Thus, the simplest way to display the planet detection sensitivity to is to give the number of expected planet detections under the assumption that each lens star has a planet of a given mass fraction, ϵ, and separation. This is what is plotted in Figs. 6 and 7. The different curves in Fig. 6 are contours of constant numbers of planet discoveries, assuming one planet per star at the given mass fraction and semi-major axis. In Fig. 7, we compare the sensitivities of the proposed GEST and STEP missions. The locations of the planets in our Solar System are also shown. Each planet name starts at the planetary mass fraction of the planet and continues toward higher mass fractions. Because the typical mass of a lens star is about $0.3\,\mathrm{M}_{\odot}$, planets of the same mass as the Solar System's planets will have a typical mass fraction that is larger by about a factor of three. A planet of one Earth mass, for example, will usually have $\epsilon \approx 10^{-5}$ rather than $\epsilon = 3 \times 10^{-6}$, which is the Earth's mass fraction. So, the sensitivity to planets with the same mass as those in the Solar System will appear near the top of each planet name while the bottom of each planet name indicates the sensitivity to planets of a fixed mass fraction. The sensitivity to planets of $1\,\mathrm{M}_\oplus$ for the parameters of the GEST mission is shown in Figure 8 which indicates that just over 100 Earths would be detected if each lens star has one in a $1\,$AU orbit. The peak sensitivity is at an orbital distance of $2.5\,$AU where we would expect 230 detections if each lens star star had a planet in such an orbit.

The green and yellow shaded regions in Figure 6 indicate the sensitivity of other planet search techniques. The known extra-solar planets which orbit main sequence stars have been discovered with the precision radial velocity technique (Marcy & Butler 1996), and a number of these individual detections are indicated in the upper left region of the figure at small semi-major axes and large masses. The solid yellow shaded region indicates the sensitivity of a 20-year radial velocity program assuming a minimum detectable velocity amplitude of $10\mathrm{m/sec}$. This is close to the demonstrated accuracy of the Keck (Marcy & Butler 1996) and CORALIE (Queloz et al. 2000) radial velocity programs, but it is expected that the current radial velocity state of the art is close to the limit set by the intrinsic radial velocity noise of the source stars. The expected sensitivity of the planned 5-year Space Interferometry Mission (SIM) satellite is shown in green with the vertical green lines showing the planned SIM sensitivity and the solid green region showing the sensitivity of the SIM floor mission. (The assumed detectable astrometric signals are $1\,\mu$as and $6\,\mu$as, respectively, at a distance of $10\,$pc.)

The cyan shaded region in Figure 6 represents the space-based transit technique which is very sensitive to terrestrial planets in short period orbits. Several such transit missions are planned including the French COROT mission, ESA's (not yet funded) Eddington mission, and NASA's Kepler mission. Kepler will be the most sensitive of these, and its sensitivity is represented by the diagonal cyan lines. A sensitive transit search like Kepler is the only program that is competitive with a space-based microlensing survey for finding Earth-mass planets at $1\,$AU. However, the prime sensitivity of a transit survey extends inwards from $1\,$AU, while the sensitivity of microlensing extends outwards. So, the two methods are largely complementary.

Figs. 6 indicates that microlensing's peak planet detection sensitivity is at 2-3 AU with significant sensitivity in the range 0.7-10 AU. In fact, the sensitivity at large distances is underestimated by our simulation because we do not consider planets that may be detected when the source star magnification is $A < 1.06$. Events with $A_{\max} < 1.06$ and events with the planetary deviation which occurs before or after the $A > 1.06$ region of the light curve have not been included in our simulations. However, some of these planets will be detectable. A lower limit on our sensitivity to distant planets is set by our sensitivity to free-floating planets which is discussed in section 3.6. This sensitivity is indicated by the thinner, horizontal lines on the right side of Figure 6. These lines should be considered to extend to infinite distances, indicating that a space-based microlensing survey has strong sensitivity to planets at separations of $0.7\,$AU to ∞. However, for planets at distances $\gg 10\,$AU, it will often be the case that the star that the planet orbits will not be detectable. Such cases may be difficult to distinguish from free-floating planet detections unless the lens star can be detected (see Section 3.7).

Microlensing of Galactic bulge stars is most sensitive at semi-major axes of 2-3 AU because this is the typical Einstein ring radius for Galactic bulge source stars. Images are located close to the Einstein ring when they are bright, and the a planet is most easily detectable if one of the bright images passes close to it. In contrast, the astrometry technique is more sensitive at large orbital radii, while the radial velocity and transit techniques (see section 3.9) are more sensitive at smaller radii. The astrometry, radial velocity, and transit techniques all have sharp cutoffs on their sensitivity at larger semi-major axes due to the fact that these techniques require data from a full orbit, or several orbits in the case of transits. Thus, microlensing has an advantage over these other techniques at large orbital distances, since it is able to make prompt discoveries of distant planets.

The main advantage of the microlensing technique over both the astrometry and radial velocity techniques is its sensitivity to lower mass planets. At 1 AU, microlensing is sensitive to planets with masses that are about three orders of magnitude smaller than the smallest masses that ground based radial velocity and astrometry searches are likely to detect. A space based microlensing survey also offers an advantage in sensitivity to low mass planets with respect to space based astrometry missions such as SIM. Figure 6 indicates that GEST's sensitivity extends to masses that are a factor of 20 lower than expected for the SIM baseline mission and a factor of 100 lower than for the SIM floor mission. (The floor mission is considered to be the minimum acceptable sensitivity that SIM could descope to if it should run into budget problems.) Of course, SIM will find planets orbiting nearby stars, so planetary results to be expected from the GEST and SIM missions are somewhat complementary: GEST will determine extrasolar planet abundances extending down to very low masses, while SIM will study planetary systems close to the Sun with sensitivity down to planets somewhat more massive than the Earth.

Another important advantage of the gravitational microlensing technique is that the low mass planets are detected with high signal-to-noise. In fact, for a large range of planetary masses, the strength of the microlensing signal does not depend on the mass of the planet. Low mass planets do affect a smaller region of the lens plane, so they have a lower detection probability and a shorter duration. Figure 9 shows the distribution of the signal-to-noise of our detected planets for planetary mass fractions ranging from $\epsilon = 3 \times 10^{-7}$ (Mars-like) to $\epsilon = 3 \times 10^{-4}$ (Saturn-like). $\Delta\chi^2$ is the detection significance parameter used for the x-axis of this plot, and a logarithmic scale must be used because of the large spread in $\Delta\chi^2$ values. The most striking feature of this figure is that number of events with large $\Delta\chi^2$ values falls off rather slowly. The power law, $N \sim \left(\Delta\chi^2\right)^{-1.3}$, provides a rough fit to these curves for all but the lowest mass fraction ($\epsilon = 3 \times 10^{-7}$) where the effects of the finite angular size of the source stars begin to reduce the number of high signal-to-noise events.

3.4. Sensitivity Dependence on Telescope Parameters

Tables 1 and 2 summarize how the planet detection sensitivity for Earth-like planets depends on the parameters of the space-based microlensing survey telescope. The parameters varied are the telescope field of view, the assumed minimum photometric error in a 10 minute exposure, the assumed FWHM of the images, and the effective telescope aperture in meters. The FWHM and aperture are considered independently because they can be varied independently when the pass-band and telescope optics are varied. The pass-band and detector sensitivity contribute to the effective aperture by modifying the total number of photons detected. The effective aperture is normalized assuming the detector quantum efficiency of the standard CCDs shown in Fig. 2 with a broad 0.5-$0.9\,\mu$ pass-band and a telescope optical thruput of 70%. Narrower pass-bands can decrease the effective aperture, and the use of more sensitive detectors can increase the effective aperture. Thus, the telescope proposed for the GEST MIDEX proposal has an effective aperture of 1.25m even though the actual aperture is 1.0m because the more sensitive Lincoln Labs CCDs are used with a 0.5-$1.0\,\mu$ pass-band.

The planet detection sensitivity has a weaker dependence on a number of these parameters than might naively be expected. For example, the number of planets detected does not depend linearly on the field-of-view because we are able to select a field with a higher average microlensing optical depth when the field is smaller. Also, the dependence on the image FWHM is relatively weak because all of the values considered allow stars near the top of the bulge main sequence to be individually resolved. The sensitivity decreases quite substantially at FWHM $\gtrsim 0.5$", however.

We should caution that the main advantage of a more sensitive telescope, like the proposed STEP mission, is the increased sensitivity to multiple planet detections. As described in sub-section 3.2.1, the proposed STEP mission should expect to detect 3-3.5 times more multiple planet systems than the proposed GEST mission would. Some of this increase in sensitivity to multiple planets is due to the fact that the probability of detecting two planets scales like the single planet detection probability squared. However, when one planet is detected, it often has a separation that is close to the Einstein ring radius. Since a second planet is likely to have a separation that is not close to the Einstein ring radius, it will likely have a weaker than average signal. Thus, the ability to detect multiple planets is more sensitive to the telescope size and detector sensitivity than the square of the single planet detection probability.

3.5. Variable Star Background

All of our simulations have implicitly assumed that there is no significant background of variable stars that might interfere with the detection of planets. Some justification for this is provided by the existing gravitational microlensing surveys which have not seen a significant background of variable stars (Alcock et al. 1997; Alcock et al. 2000b; Udalski et al. 2000). In fact, the most significant source of variability that might contaminate samples of gravitational microlensing events is background supernovae (Alcock et al. 2000c). However, the space-based microlensing program that we propose will use source stars that are fainter than the source stars used for the ground-based surveys. Faint flare stars (Lacy et al. 1976) are of particular concern because they can have long quiescent phases with infrequent brightenings seen in broad-band photometry. However, this broad-band variability is generally seen in the blue or ultraviolet bands, and is much less pronounced in the red and near-IR where microlensing surveys would observe.

While the ground-based microlensing surveys follow relatively bright stars in the Galactic bulge and Large Magellanic Cloud, they also observe many thousands of intrinsicly fainter stars in the foreground of these targets. None of the foreground stars observed by the MACHO Collaboration has exhibited the sort of photometric variation that could be confused with a planetary microlensing deviation if, by chance, the intrinsic stellar photometric variation occurred during a stellar microlensing event. Since we expect about 10^4 stellar microlensing events, the statistics of the foreground stars observed by the ground-based surveys suggest that there should be no contamination of the planet sample due to variable star. The data provided by a space based survey will provide much more stringent constraints on possible variable star contamination, and we expect that the accurate measurements of the light curve shape from a space-based survey will clearly distinguish between deviations due to microlensing and any intrinsic variability of the source star. It is likely that the variable star background will have a negligible effect on the sensitivity of a space-based gravitational microlensing planet search program.

3.6. Free Floating Planets

The leading theories of planet formation (Levison et al. 1998; Perryman 2000) indicate that planets often don't stay in the same orbit where they formed. The migration of giant planets inward is thought to be necessary to explain the "hot Jupiter" planets discovered by the radial velocity planet searches, and the orbital distribution of Kuiper Belt Objects (Malhotra, Duncan & Levison 2000) suggests that Neptune has migrated outward from its birth site. These migrations are likely to be due to the gravitational interactions of these giant planets with a large number of planetesimals in the protoplanetary disk. Many of these planetesimals are likely to be perturbed into highly elliptical orbits which will send them crashing into the Sun or ejecting them from the solar system, and it is expected that the most massive of these ejected objects will have a mass in the terrestrial planet range which means that they should be detectable via microlensing.

The majority of known extra-solar giant planets in orbits of semi-major axis $> 0.3\,$AU have relatively large orbital eccentricities, and this can be explained via gravitational scattering with other giant planets in the same system (Levison et al. 1998). A consequence of these interactions is that many of these giant planets will be ejected from their planetary system. Terrestrial planets, which are more easily ejected via two-body interactions, should also be ejected in large numbers. Thus, there are good theoretical reasons to believe that free-floating planets may be abundant as a by-product of the planetary formation process. If so, they can be detected via gravitational microlensing. Figure 10 shows the number of free-floating planet detections expected for the GEST mission under the assumption that there is one free-floating planet per Galactic star. The detection threshold is set higher for the free-floating planet detections because we must search $\sim 10^8$ light curves for free-floating planets while we only need to search the $\sim 10^4$ detected stellar microlensing event light curves for evidence of bound planets. Since theory predicts that many stars may be ejected from the system during the planetary formation process, it may be reasonable to assume that there will be many more free-floating planets than the numbers indicated in Figure 10. If half of the star systems eject an average of ten $1\mathrm{M}_\oplus$ planets each, then we would expect to detect more than 100. In fact, there has already been a possible detection of a free-floating planet in the MACHO data (Bennett et al. 1997).

3.7. Source Star Identification

The planets detected by and space-based microlensing survey orbit the lens stars in the foreground of the Galactic bulge source stars. The mass distribution of the lens stars from our GEST simulations is shown in Fig. 11. This distribution is somewhat flatter than the stellar mass function because we have assumed that the planetary mass distribution is proportional to the stellar mass distribution and more massive planets have a higher detection probability.

Although microlensing does not require the detection of any light from the lens stars, a significant fraction of the microlensing events seen by a space-based microlensing survey will have lens stars that are bright enough to be detected. Our simulations indicate that for $\sim$ 17% of the detected planets, the planetary host (lens) star is brighter than the source star, and for another $\sim$ 23% the lens stars that is within 2.5 I-band magnitudes of the source star's brightness. A few of these stars are blended with the images of other brighter stars, and if we ignore those stars, we find that 33% of the lens stars should be directly detectable. The detectable planetary host stars are depicted in red in Fig. 11, and they comprise virtually all of the F and G star lenses, most of the K star lenses, and a few of the nearby M-star lenses.

The visibility of the lens star will allow for the measurement of a number of other useful parameters. The most obvious of these are the apparent magnitude and color of the lens star. This would enable an approximate determination of the lens mass and distance if the dust extinction was small. Our field, however, has high and variable extinction, and so it will be prudent to obtain IR photometry. This will allow us to estimate both the extinction and the intrinsic color of the star. Because our fields are quite crowded, we will need IR observations with high angular resolution which can be obtained with adaptive optics (AO) systems on large telescope such as the VLT, Gemini, LBT or Keck. The high stellar density of the microlensing survey fields implies that there are virtually guaranteed to be nearby guide stars to provide the phase reference needed for these AO systems. We would expect to obtain two sets of IR, AO observations: one during the event which would be scheduled as soon as the planetary signal is detected and the second set of observations would be taken well after the event is over. This pair of observations taken at different lens magnifications will allow us to unambiguously determine the color and brightness of the lens stars. We will require this data only for events with detected planetary signals, and so there should no difficulty in obtaining the ground-based telescope time.

Another measurable parameter for the visible lens stars is the relative proper motion between the lens and the source which is typically $\mu \approx 8$ mas/yr for a total motion of 32 mas over 4 years. This is 15% of a CCD pixel for the sampling of the proposed GEST mission. Anderson and King (2000) argue that centroids can be measured to 0.2% of a pixel with a combination of a set of undersampled HST WFPC2 frames that have been dithered to recover the resolution lost to undersampling. A space-based microlensing survey will provide > 100 times more data than the most ambitious HST programs, which will allow numerous cross-checks to look for systematic errors in the centroid determinations. Thus, we expect that the centroids of the space-based stellar images can be determined at least as well as the centroids of the HST stars, so we expect to be able to measure the relative proper motion to an accuracy of a few percent. An independent measurement of the lens-source proper motion can be obtained for the events which exhibit planetary lens caustic crossing features. These comprise somewhat more than 50% of the events in which terrestrial planets are detected, and they allow the ratio of the angular radius of the star to the angular Einstein radius, θ_E, to be measured in the light curve fit. Since the source star angular radius can be estimated from its brightness and color, an estimate of θ_E can be obtained. The ratio of the angular Einstein radius to the lens-source proper motion is $\theta_E/\mu = t_E$, the Einstein radius crossing time which can also be measured from the light curve, and so these measurements of μ and θ_E give equivalent information.

The measurement of μ or θ_E allows us to use the following relation for the lens star mass,

$$M_l = \frac{\theta_E^2 D_s c^2}{4G} \frac{x}{1-x} \qquad (2)$$

where $x = D_l/D_s$, the ratio of the lens to source distances. This relation allows us to determine the difference between the source and lens distances when the lens is close to the source because it indicates that M_l, and hence the lens luminosity, depends sensitively on $1-x = (D_s - D_l)/D_s$. This means that the Einstein radius, R_E, can be determined for all lens stars with a measurement of the lens star brightness and its relative proper motion, μ, or its color, which in turn, implies that the planetary separation can be determined in physical units. The results of this determination are shown in Fig. 12, which shows the measured separation for detected planets as a function of their orbital semi-major axis. For this plot we have assumed that the change in the relative lens-source centroid can be measured to 2 mas, the reddening corrected I magnitude of the lens can be measured to an accuracy of 0.2 mag., and the reddening corrected I-K color can be measured to 0.1 mag. As Fig. 12, indicates, the resulting estimate for planetary semi-major axis is accurate to about 20%. The uncertainty is dominated by the unmeasured distance along the line-of-site. When the lens star cannot be detected, the projected separation between the planet and its host star can only be measured in units of R_E. This can be used to estimate the planetary orbit semi-major axis by means of the expected correlation shown in the right hand panel of Fig. 12 which indicates that physical separation can be estimated with an accuracy of a factor of 2 or 3.

3.8. Measurable Planetary Parameters

The utility of planets that are detected by a space-based gravitational microlensing survey depends, of course, on the planetary properties that can be measured. For the $\sim 33\%$ of events with lens stars that are bright enough to be detected, the following parameters can be measured:

- The mass of the planetary host (and lens) star is determined (with some redundancy) from the microlensing event time scale, the lens-source proper motion, μ, and the source brightness and color.
- The planetary mass, $M_{\rm planet}$, is determined from the the stellar mass and planetary mass fraction, ϵ, which comes from the microlensing light curve fit.
- The distance to the planetary host star is determined from the same combination of parameters that gives the stellar mass.
- The planet-star separation (in the plane of the sky) is always measured in units of the Ein-

stein ring radius, R_E. This can be converted to physical units when the lens star is detected.

For the remaining events with undetectable primary stars, the measurable parameters are the following:

- The planetary mass fraction, $\epsilon = M_{\rm planet}/M_*$, is determined from the microlensing light curve.
- The planet-star separation is measured in units of the Einstein ring radius, R_E, and this can be converted to physical units with an accuracy of a factor of ~ 2.
- The masses of the free-floating planets must generally be determined from the event time scale only. This can be done to an accuracy of a factor of three for each individual event.
- Many of the $\sim 1\,{\rm M}_\oplus$ planets and virtually all of the $\sim 0.1\,{\rm M}_\oplus$ planets detected will have caustic crossing features which depend on the ratio of the source star radius to R_E. This will allow a mass estimate with an accuracy of a factor of two for planets orbiting a star or detected as isolated objects.

3.9. Planet Detection via Transits

While the focus of the space mission that we propose is to find low mass planets via gravitational microlensing, the survey will also be sensitive to giant planets via transits of the $\sim 10^8$ Galactic bulge stars being monitored. Since giant planets like Jupiter have a radius that is about 10% of a solar radius, a transit of a Jupiter-like planet across the Sun will reduce the apparent brightness of the Sun by about 1%. The proposed GEST telescope has the sensitivity to detect such a transit of a solar-type Galactic bulge star by a Saturn size planet, and the following argument shows that such a mission can detect transits of Saturn size planets orbiting fainter main sequence stars, as well. The luminosity and radius of a main sequence star obeys the following approximate relations: $L \propto M^{3.5}$ and $R \propto M$. Since the fractional photometric signal from a transiting planet (of a fixed radius) goes as R^{-2}, the signal-to-noise for a transiting planet scales as $M^{-0.25}$, which is a very weak dependence slightly favoring lower mass stars.

Some of the $\sim 10^8$ target stars will have images that are blended with those of their near neighbor stars, and this can cause a substantial increase in the photon noise which significantly reduces the sensitivity to planetary transits. This effect has been included in our calculations of the expected numbers of detectable planetary transits. The number of expected planetary transit detections for planets at different orbital distances are summarized in Table 1 which assumes a detection threshold of a 6.5σ detection of a planet of Saturn's radius in 5 hours of exposures. This translates into a 9σ detection of a Jupiter sized planet. A crucial ingredient of our transit detection calculation is the inclusion of realistic stellar radii for the source stars, because many of them have a radius that is substantially smaller than the Sun.

Planets with orbital periods longer than 4 years can be detected via transits, but only one transit will be detected per planet. Such transits should have enough signal-to-noise for a significant detection because the transit duration is $\gtrsim 10$ hours, but the period of the planet can only be roughly estimated from the transit duration. Because of the huge number of stars that will be observed, planets out to ~ 20 AU are detectable even though there is only a probability of $\sim 2 \times 10^{-6}$ that such a planet would have its orbit aligned with the line of sight and have the right orbital phase to transit the source star during the period of observations. This sensitivity to distant planets via transits means that a space-based microlensing planet search mission will have a very substantial overlap in the planetary separations probed by the microlensing and transit techniques. At orbital distances of 0.4-20 AU, the proposed GEST mission will be sensitive to giant planets through both methods. This will allow cross-checks to help confirm the planetary interpretation of the transits. Since the transit signal indicates radius rather than mass, some of the transits could be caused by low mass M-dwarfs or brown dwarfs with similar radii, but much larger masses than giant planets. Thus, some form of confirmation is desirable. For example, we might measure the radial velocities of some sub-sample of the candidate planets detected via transits using a moderate resolution multi-object spectrograph. This would not allow us to distinguish between giant planets and low-mass brown dwarfs, but we should detect radial velocity variations for for those stars which are transited by M-dwarfs or high-mass brown dwarfs. This might allow a statistical correction for the non-planetary transits.

With the combined sample of microlensing and transit detections of giant planets, a wide FOV space telescope will be able to probe the entire range of giant planet orbital radii: from 0, where the transit technique is very efficient, to ∞, where microlensing is the only viable technique. Thus, such a telescope promises a complete survey of giant planets with the combination of the two techniques.

3.10. Additional Science with a wide FOV Space Telescope

There are several other space-based microlensing planet search capabilities that we have not discussed in detail. Planets orbiting a single star of a binary system have been detected via radial velocities (Marcy & Butler 1996), and gravitational microlensing evidence has been presented for a planet orbiting a binary star system (Bennett et al. 1999), although this interpretation remains uncertain (Albrow et al. 2000a) due to incomplete coverage of the microlensing light curve.

An additional capability that we have not discussed in this paper is the possibility of studying the abundance of planets in external galaxies, such as M31 (Covone et al. 2000). While most of the source stars in M31 will be either poorly resolved or unresolved by a telescope with angular resolution that is no better than that of HST, it is still possible to detect microlensing events with giant star sources if the microlensing magnification is not too small. Because an M31 planet search follows mostly giant source stars, it will not be very sensitive to terrestrial extra-solar planets, but it should be able to a detect large number of giant planets at a separation of 1-10 AU and measure their abundance as a function of position in the galaxy.

Other possible science programs include a high redshift supernovae search and a deep, wide-field, high resolution weak lensing survey. (Both of these are goals of the proposed SNAP mission.) It would also be possible to carry out a deep Kuiper Belt Object (KBO) search which should discover 100,000 new KBOs (Cook et al. 2000). Many of these programs could be carried out during the 4 months per year when the Galactic bulge planet search field is too close to the Sun to be observed, and they might be selected as a part of a general observer program via a competitive review.

4. Conclusions

In this paper, we have presented the results of a simulations of a space-based gravitational microlensing survey for terrestrial extra-solar planets, similar to the proposed GEST mission. We have determined the expected planet detection sensitivity as a function of the planetary mass fraction, ϵ, and the orbital semi-major axis, and we have shown how the sensitivity to Earth-like planets depends on the telescope parameters. We have found that such a mission will be sensitive to planets down to a tenth of an Earth mass, or about 1000 times less than the masses of planets discovered with the radial velocity technique.

We have shown that a space-based microlensing planet search program should be able to directly detect the planetary host (and lens) stars for about one third of the detectable planets. The observations of the host star when combined with the microlensing light curve will allow the determination of the planetary mass and separation as well as the stellar mass, type, and Galactocentric distance. The visible stars include virtually all of the "solar type" lens stars, *i.e.* those of spectral type F, G, or K which comprise about 25% of the total. For the remainder of the lens stars, which are mostly M-dwarfs, it is generally possible to accurately determine the planetary mass fraction and to determine the projected planet-star separation to an accuracy of a factor of 2. For about one third of the detected planets, the lens star should be directly detectable in the space-based survey data and with ground-based infrared observations (with adaptive optics). This allows an accurate determination of the mass and distance to the primary as well as the planetary separation in physical units.

The expected scientific output of a space-based microlensing planet search program is summarized here:

- The average number of planets per star down to $0.1\,\mathrm{M}_\oplus$ at separations of $\sim 0.7\,$AU - ∞ for terrestrial planets and 0 - ∞ for giant planets.
- The planetary mass function as a function of the planetary mass fraction, $f(M_{\rm planet}/M_*)$, and separation, for all lens stars.
- The planetary mass function as a function of stellar mass, Galactocentric distance, and the planet-star separation for G, K, and early M stars.
- The abundance of giant planet pairs. A high abundance will indicate a large fraction of near circular orbits.
- The ratio of free-floating to bound planets as a function of planetary mass.

Finally, we would like to emphasize that the results that we have presented are based upon very conservative assumptions. We've assumed a microlensing optical depth number that is 1.3 times smaller than the latest measurements indicate. If we assume that the optical depth measurement errors have a normal distribution, this is the 95% confidence level lower limit on the microlensing optical depth.

We've also been conservative in the selection of our planet selection criteria by demanding a 12.5σ improvement ($\Delta\chi^2 \geq 160$) for a planetary microlensing fit compared to a single lens fit. This ensures that we can make a reasonably accurate determination of the planetary parameters, but the event count could probably by increased by about 70% if the threshold was dropped to 9σ. Furthermore, events with a peak magnification $A_{\rm max} > 200$ have not been included because they may be difficult to interpret. All told, if we dropped all of our conservative assumptions, we would have an event rate that is 2-3 times higher than we have reported (although the interpretation of some of these events might be difficult).

In summary, we've demonstrated that the a space-based microlensing planet search mission can detect planets with masses down to that of Mars which is a tenth of and Earth mass and some three orders of magnitude better than current techniques. Space-based microlensing is unique among indirect terrestrial planet search programs in that low mass planets are detected at high signal-to-noise. Such a mission would be sensitive to terrestrial planets at orbital distances of $\gtrsim 0.7\,$AU via microlensing as well as giant planets are all orbital radii via both microlensing and transits. If each star has a $1\,\mathrm{M}_\oplus$ planet orbiting at 1 AU, GEST would detect ~ 100 of these. For about one third of the detected planets, the host stars would be directly observable in the images. This will allow the determination of the stellar type, mass, and distance, and it will allow an accurate estimate of the planet-star separation in AU. The results we've presented indicate that a space-based microlensing planet search program could provide very useful statistics on the abundance of terrestrial and giant planets well in advance of the Terrestrial Planet Finder (TPF) mission, and this information would likely be quite useful in planning TPF.

Acknowledgments

We'd like to thank John Mather for encouragement and advice during the early stages of this work, and we'd also like to thank Domenick Tenerelli and his team at Lockheed Martin Space Systems for their efforts on behalf of the GEST Discovery proposal. Finally, we'd like to thank the GEST Co-Investigators for their help. The Co-Investigators are: I. Bond, E. Cheng, J. Connor, K. Cook, P. Garnavich, K. Griest, D. Jewitt, N. Kaiser, T. Lauer, J. Lunine, G. Luppino, D. Minniti, S. Peale, M. Shao, R. Stevenson, C.

Stubbs, N. Woolf, and P. Yock. This work was supported, in part, by the NASA Origins Grants NAG5-4573 and NAG5-9731.

REFERENCES

Albrow, M. D., et al. 2000a, ApJ, 534, 894.

Albrow, M. D., et al. 2001, ApJ, 556, L113.

Albrow, M. D., et al. 2000b, ApJ, 535, 176.

Alcock, C., et al. 1997, ApJ, 479, 119; (E) 500, 522

Alcock, C., et al. 2000, ApJ, 541, 270

Alcock, C., et al. 2000, ApJ, 541, 734

Alcock, C., et al. 2000, ApJ, 542, 281

Anderson, J. & King, I. R. 2000, PASP, 112, 1360

Beichman, C. 1998 Terrestrial Planet Finder: The Search for Life-Bearing Planets Around Other Stars SPIE, 3350, 719

Bennett, D. P., et al. 1997, ASP Conf. Proc. 119: Planets Beyond the Solar System and the Next Generation of Space Missions, D.R. Soderblom, ed., p. 95. (astro-ph/9612208)

Bennett, D. P., & Rhie, S. H., 1996, ApJ, 472, 660.

Bennett, D. P., & Rhie, S. H., 2000, Proc. of the Disks, Planetesimals & Planets Meeting held in Tenerife, Jan. 24-28, 2000, (astro-ph/0003102)

Bennett, D. P., & Rhie, S. H., 2002, in preparation

Bennett, D. P., et al. 1999, Nature, 402, 57.

Bennett, D. P., et al. 2000, BAAS, vol. 32, no. 3, p. 3206; (also at http://bustard.phys.nd.edu/GEST/publications.html)

Bertelli, G., Bressan, A., Chiosi, C., Fagotto, F., & Nasi, E. 1994, A&AS, 106, 275

Bissantz, N., Englmaier, P., Binney, J., & Gerhard, O., 1997, MNRAS, 289, 651

Bolatto, A. D., & Falco, E. E. 1994, ApJ, 436, 112

Butler, R. P. & Marcy, G. W., 1996, ApJ, 464, L153

Carr, M. H. (1996) Water on Mars, Oxford University Press, New York.

Chyba, C. F., et al. 2000, ”Planetary habitability and the origin of life,” In Protostars and Planets IV (V. Mannings, A. P. Boss, and S. Russel, Eds.), pp. 1365-1393. University of Arizona Press, Tucson.

Cook, K. H., et al. 2000, BAAS, vol. 32, no. 3, p. 2101; (also at http://bustard.phys.nd.edu/GEST/publications.html)

Covone, G., de Ritis, R., Dominik, M., Marino, A. A., et al. 2000, A&A, 357, 816

Danner R, Unwin S 1999 *SIM: Taking the Measure of the Universe* NASA/JPL

Deeg, H. J., et al. 2000, ASP Conf. Proc., in press: Planetary Systems in the Universe: Observation, Formation and Evolution (IAU Symp. 202), Penny, Artymowicz, Lagrange and Russell, eds. (astro-ph/0011143)

Des Marais, D. J., et al. 2001, Jet Propulsion Laboratory publication: JPL 01-008.

di Stefano, R., & Esin, A. A., 1995, ApJ, 448, L1

Dominik, M. 1999, A&A, 341, 943

Dressler, A., et al. 1996, “HST and Beyond; Exploration and the Search for Origins: A Vision for Ultraviolet-Optical-Infrared Space Astronomy,” AURA publication, available at: http://www.stsci.edu/stsci/org/hst-and-beyond-report.pdf

Fridlund, C.,V., M. 2000 Darwin: the Infrared Space Interferometer in B Schürmann, ed., *Darwin and Astronomy* 11–18 ESA SP–451, Noordwijk, NL

Gaudi, B. S., & Gould, A. 1997, ApJ, 486, 85

Gaudi, B. S., Naber, R. M. & Sackett, P. D. 1998, ApJ, 508, L33

Gaudi, B. S. 1998, ApJ, 506, 533

Gilliland, R. L., et al. 2000, ApJ, 545, L47

Gould, A., & Loeb, A. 1992, ApJ, 396, 104

Griest, K. & Safizadeh, N. 1998, ApJ, 500, 37

Han, C. 1997, ApJ, 490, 51

Han, C. & Gould, A. 1997, ApJ, 480, 196

Holtzman, J. A., et al. 1998, AJ, 115, 1946

Kasting, J. F. 1997, Origins of Life 27, 291-307.

Kasting, J. F.., Whitmire, D. P., and Reynolds, R. T. 1993, Icarus 101, 108-128.

Koch, D. G., et al. 1998, SPIE, 3356, 599

, Kepler web site: http://www.kepler.arc.nasa.gov/

Kroupa, P., & Tout, C. A. 1997, MNRAS, 287, 402

Kroupa, P. 2000, International Conference of the Astronomische Gesellschaft, vol. 16, p. 11

Lacy, Lacy, C. H., Moffett, T. J., & Evans, D. S. 1976, ApJS, 30, 85

Lauer, T. R. 1999, PASP, 111, 1434

Levison, H. F., Lissauer, J. J., Duncan, M. J. 1998, AJ, 116, 1998

Lunine, J. I. 1999, *Earth: Evolution of a Habitable World*, (Cambridge University Press, Cambridge, U.K.)

Lunine, J. I. 2001, Proc. Nat. Acad. Sci., 98, 809

Malhotra, R., Duncan, M. J. & Levison, H. F. 2000, in Protostars and Planets IV, eds Mannings, V., Boss, A.P., Russell, S. S., p. 1231

McKee, C. F., Taylor, J. H., (eds.) 2000, "Astronomy and Astrophysics in the New Millennium," National Academy Press, Washington, D. C.

Mao, S., & Paczyński, B. 1991, ApJ, 374, L37

Marcy, G. W., & Butler, R. P. 1996, ApJ, 464, L147

Marcy, G. W., & Butler, R. P. 2000, PASP, 112, 137

Marcy, G. W., Cochran, W. & Mayor, M. 2000, in Protostars and Planets IV, eds Mannings, V., Boss, A.P., Russell, S. S., p. 1285

Mayor, M., & Queloz, D. 1995, Nature, 378, 355

Peale, S. J. 1997, Icarus, 127, 269

Peale, S. J. 1998, ApJ, 509, 177

Perryman, M. A. C. 2000, Rep. Prog. Phys., 63, 1209 (astro-ph/0005602)

Popowski, P., et al. 2000, preprint (astro-ph/0005466)

Queloz, D., et al. 2000, A&A, 354, 99

Rhie, S. H., et al. 2000, ApJ, 533, 378

Rhie, S. H., et al. 2000b, BAAS, vol. 32, no. 3, p. 3210; (also at http://bustard.phys.nd.edu/GEST/publications.html)

Sackett, P. D., 1997, Appendix C of ESO Document: SPG-VLTI-97/002: "Final Report of the ESO Working Group on the Detection of Extrasolar Planets," (astro-ph/9709269).

Sackett, P. D., et al. 1999, Planets Outside the Solar System: Theory and Observations, J.-M. Mariotti and D. Alloin, eds., p. 189

Schneider, J., Auvergne, M., Baglin, A., et al. 1998 The COROT Mission: From Structure of Stars to Origin of Planetary Systems in Woodward, Shull, Thronson, eds., *Origins* ASP Conf. Series 148 298–303 San Francisco

Schechter, P. L., Mateo, M. & Saha, A. 1993, PASP, 105, 1342

Schlegel, D. J., Finkbeiner, D. P. & Davis, M. 1998, ApJ, 500, 525

Stanek, K. Z. 1999, ApJ, submitted (astro-ph/9802307)

Tytler, D. 1996, in “A Road Map for the Exploration of Neighboring Planetary Systems (ExNPS),” Chap. 7, available at http://origins.jpl.nasa.gov/library/exnps/ExNPS.html

Udalski, A., Szymanski, M., Kaluzny, J., Kubiak, M., Krzeminski, W., Mateo, M., Preston, G. W., & Paczyński, B. 1994, Acta Astronomica, 44, 165

Udalski, A., Zebrun, K. Szymanski, M., Kubiak, M., Pietrzynski, G. Soszynski, I., & Wozniak, P., 2000, Acta Astronomica, 50, 1

Ward, W. R. 1982, Icarus, 50, 444

Ward, P., & Brownlee, D. 2000, *Rare Earth*, (Copernicus, New York).

Wambsganss, T. R. 1997, MNRAS, 284, 172

Wozniak, p., & Paczyński, B. 1997, ApJ, 487, 55

Zoccali, C., et al. 2000, ApJ, 530, 418

This 2-column preprint was prepared with the AAS LaTeX macros v4.0.

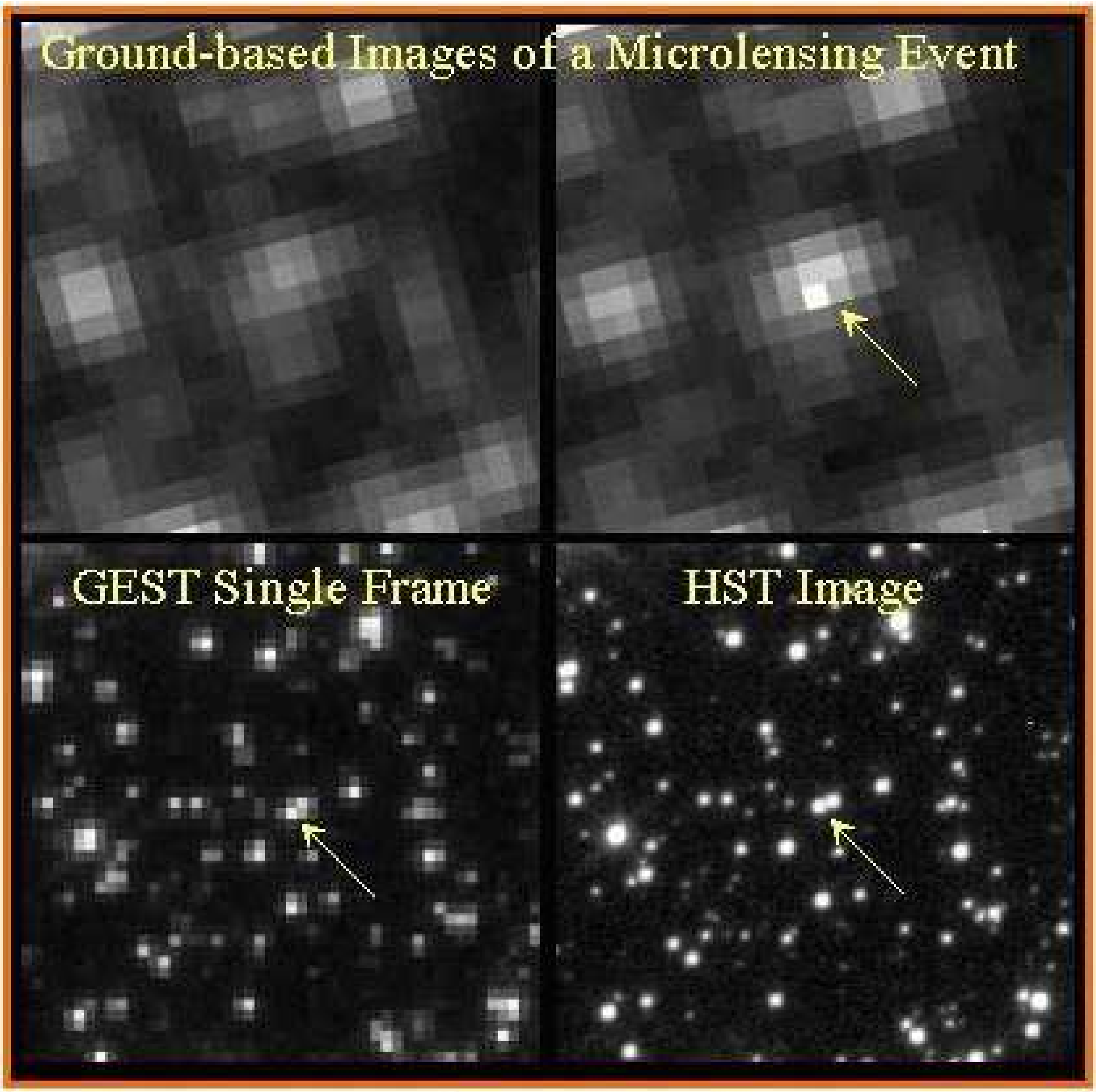

Fig. 1.— The difference between ground and space-based data for microlensing of a bulge main sequence star is illustrated with images of microlensing event MACHO-96-BLG-5. The two top panels are 50 min. R-band exposures with the CTIO 0.9m telescope taken in 1" seeing at different microlensing magnifications, and the two images on the bottom have been constructed from HST frames. The bottom left image represents a 10 minute exposure with GEST's angular resolution and pixel size, and the image on the right is an HST image. The lensing magnification factors are A = 4 and 10 for the ground based images and 1.07 for the space based image. The source star, a Galactic bulge G-dwarf is indicated by the yellow arrows.

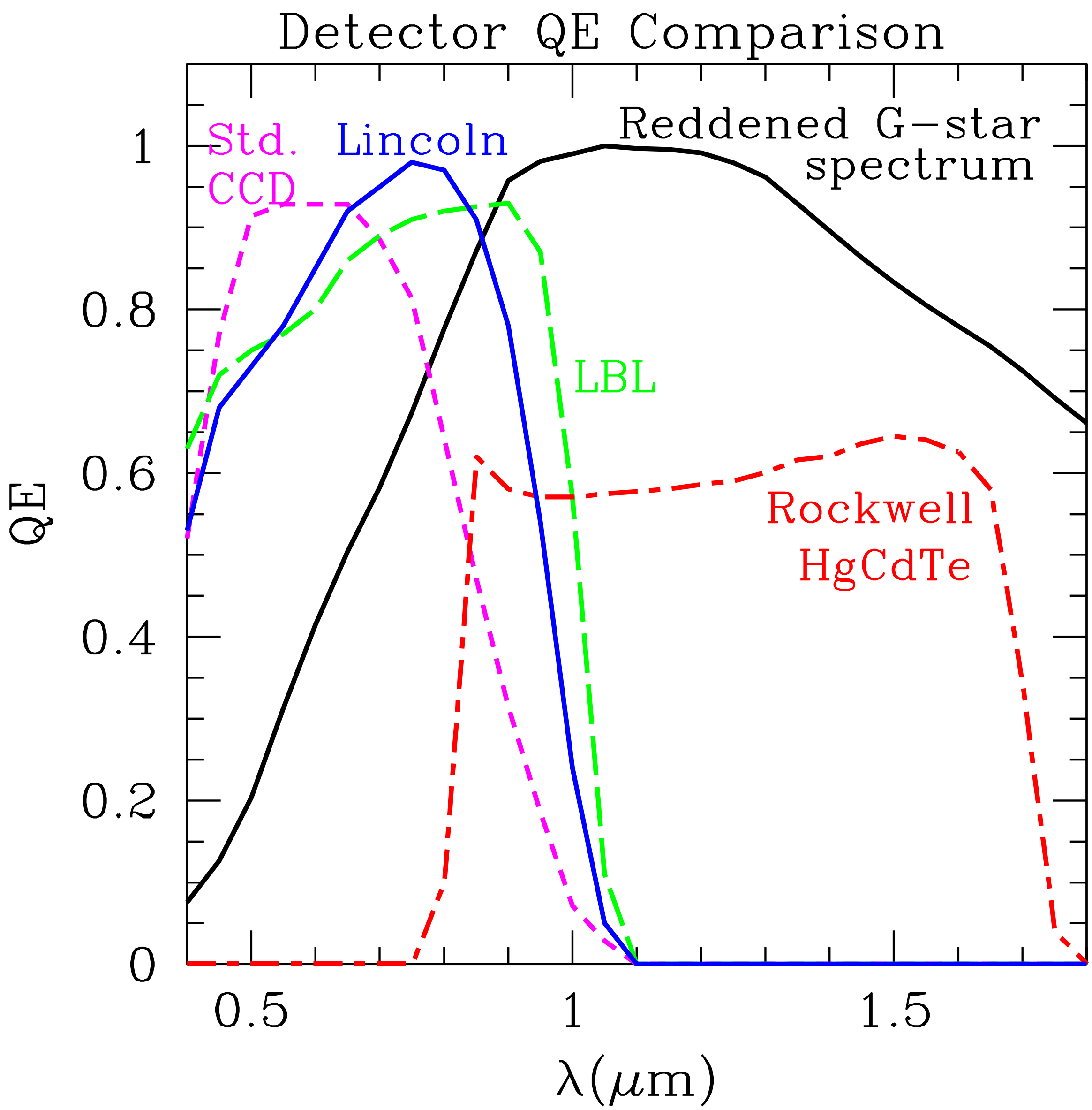

Fig. 2.— The spectrum of a typical reddened, Galactic bulge source star is compared to the quantum efficiency curves for detectors that might be used for a microlensing planet search program. The Std. CCD curve represents a Marconi CCD, which has a QE curve similar to the CCDs that are currently being produced by Fairchild and SITe as well as Marconi. The Lincoln Labs and LBL CCDs use high resistivity Silicon for enhanced sensitivity in the near IR, and the Rockwell device is one designed for HST's upcoming Wide Field Camera 3.

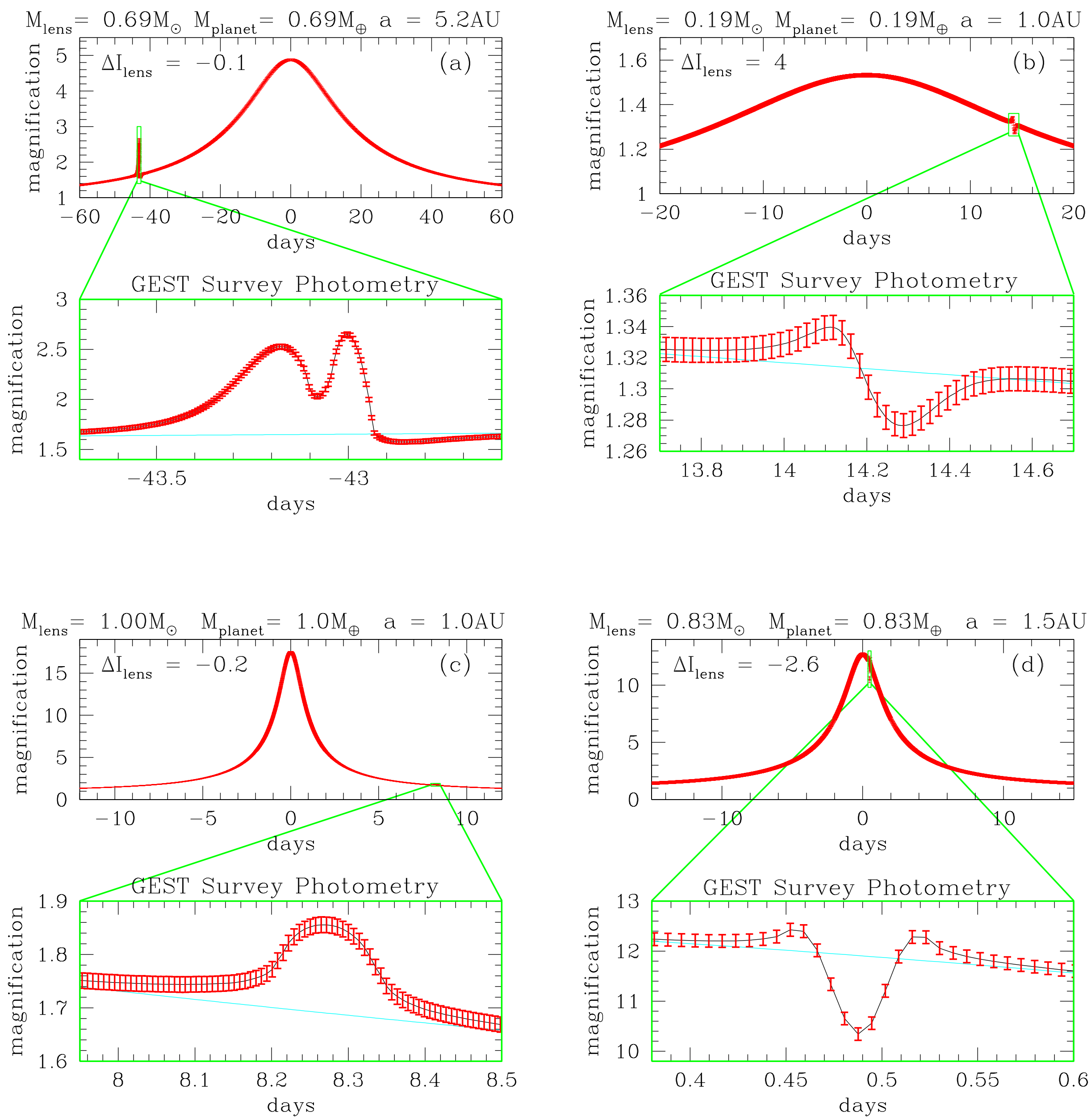

Fig. 3.— Example light curves are shown from a simulation of the GEST mission. In each case, the top panel shows the full light curve, and the planetary deviation regions are blown up and shown in the lower panels. All of the example light curves have the Earth:Sun mass ration of $\epsilon = 3 \times 10^{-6}$. Figs. (a) and (b) span the range of planetary detection significance from $\Delta\chi^2 = 60,000$ (a) to $\Delta\chi^2 = 180$ (b) which is close to our cut. Figures (c) and (d) show more typical light curves with $\Delta\chi^2 = 3000$ and $\Delta\chi^2 = 500$, respectively. The planets detected in (b) and (c) have orbital radii of 1 AU while the events shown in (a) and (d) have orbital radii of 5 and 1.5 AU, respectively. ΔI_{lens} is the difference between lens and source I magnitude.

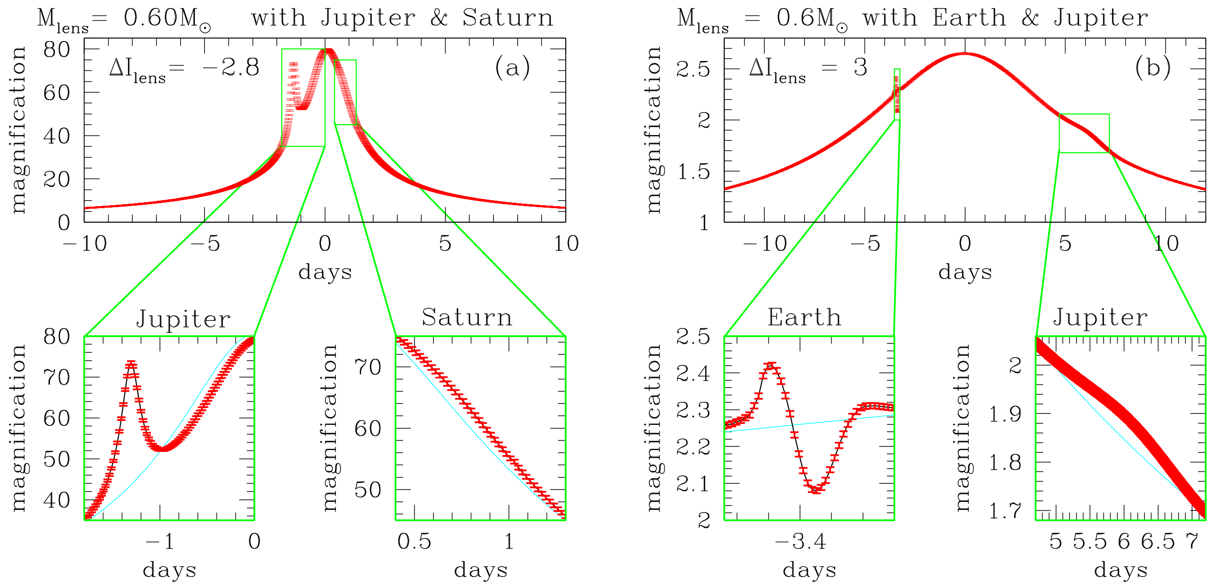

Fig. 4.— Example multiple planet light curves from our simulation of planetary systems with the same planetary mass ratios and separations as in our solar system. (a) is an example of a Jupiter/Saturn detections and (b) is an example of the detection of Earth and a Jupiter.

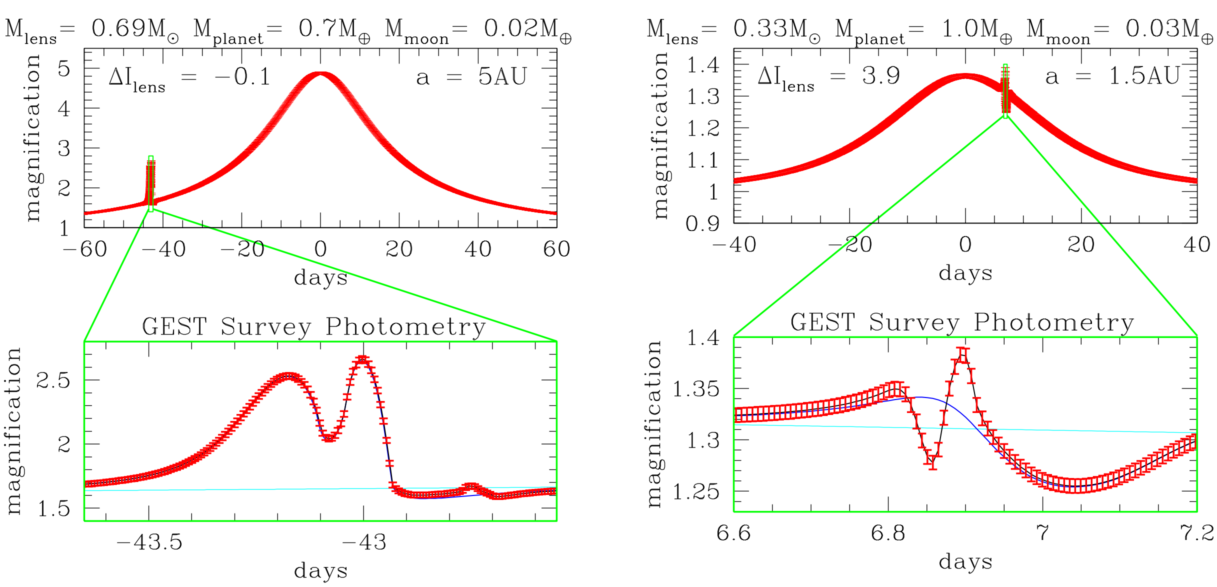

Fig. 5.— Example light curves of terrestrial planets with moons which have 1-2 times the mass of the Earth's moon. These moons orbit at 3.3 and 0.56 times the Earth-moon separation, respectively.

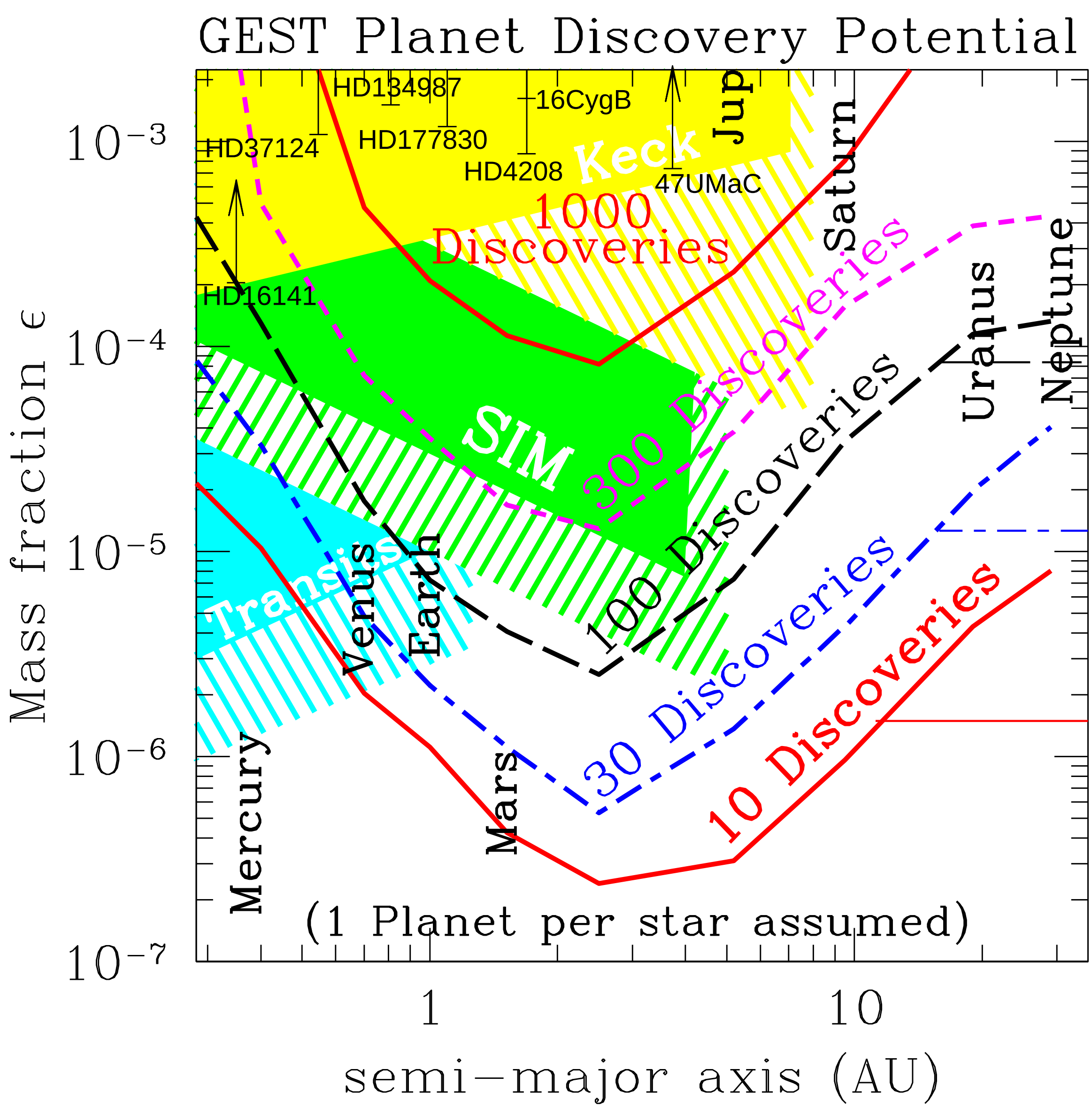

Fig. 6.— The sensitivity of the proposed GEST mission is plotted as a function of planetary mass fraction, ϵ, and orbital semi-major axis. The curves are contours indicating the expected number of GEST planet discoveries assuming 1 planet per star with the given parameters. The solid yellow region gives the sensitivity of a 20-year radial velocity program on the Keck Telescope assuming a detection threshold of 10 m/sec, and the yellow lines indicate the sensitivity of a 10-year interferometric astrometry program with a 30 μas detection threshold. The green regions indicate the sensitivity of the SIM recommended and floor missions. The location of our Solar System's planets and some of the extra-solar planets detected by radial velocities are shown. Most detected Earth mass planets have $\epsilon \approx 10^{-5}$ because the typical lens star has a mass of $\sim 0.3 M_\odot$, so the plot indicates that GEST can see ~ 35 Earth-mass ratio planets at 1 AU and ~ 100 Earth-mass planets at that distance. The horizontal lines indicate the sensitivity to free-floating planets since the more distant planets can sometimes be detected without seeing a microlensing signal from their star.

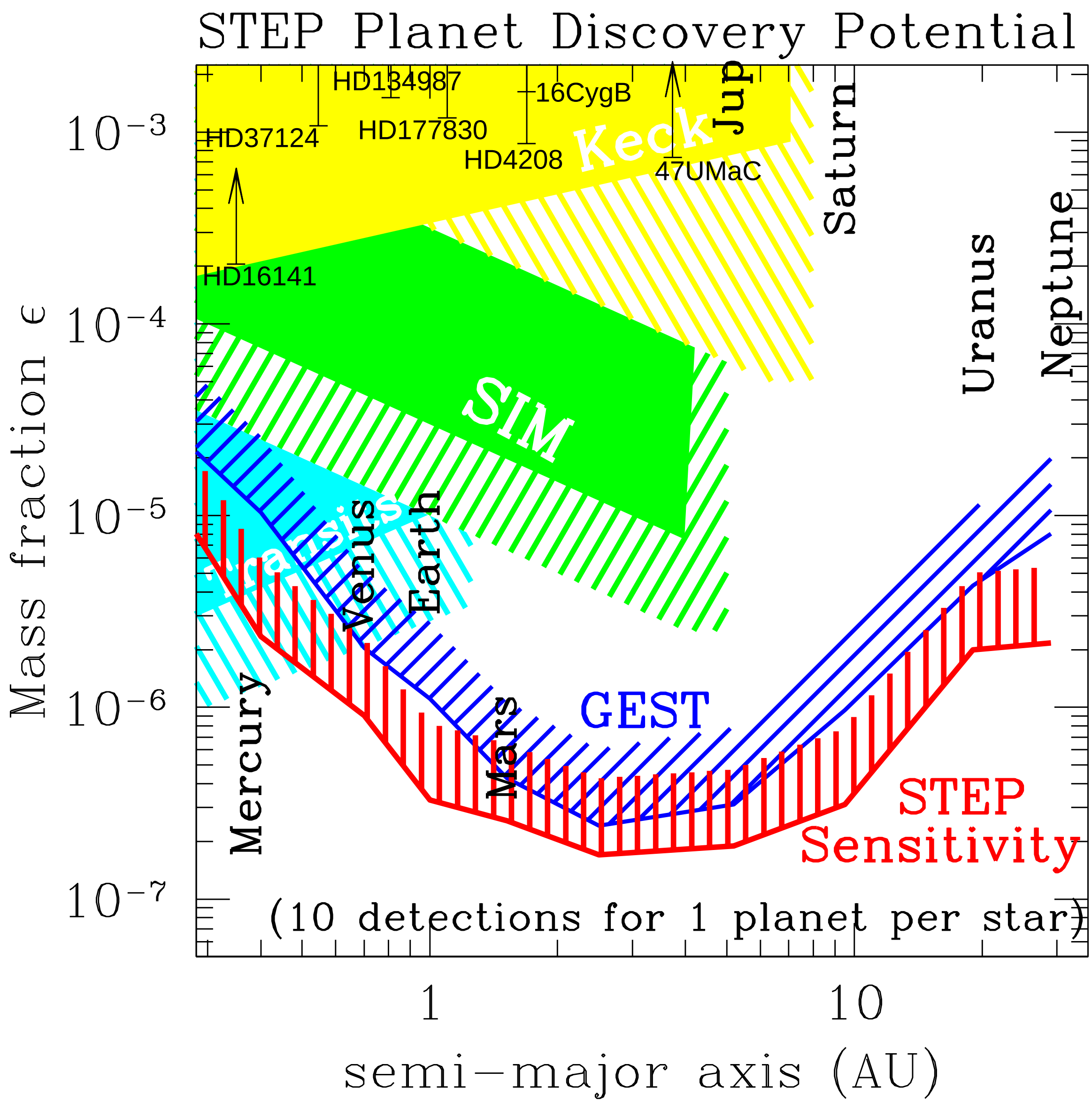

Fig. 7.— The sensitivity of the more ambitious STEP mission sensitivity is compared to the sensitivity of the proposed GEST mission, as well as the other planet search techniques shown in Fig. 6. The improvement in sensitivity due to STEP's larger telescope and more sensitive detectors is more pronounced at large and small separations than at the region of maximum sensitivity at 2-3 AU. This is because the more sensitive mission is able to detect planetary signals of a smaller amplitude which often occur for planets with separations that are significantly smaller or larger than the Einstein ring radius.

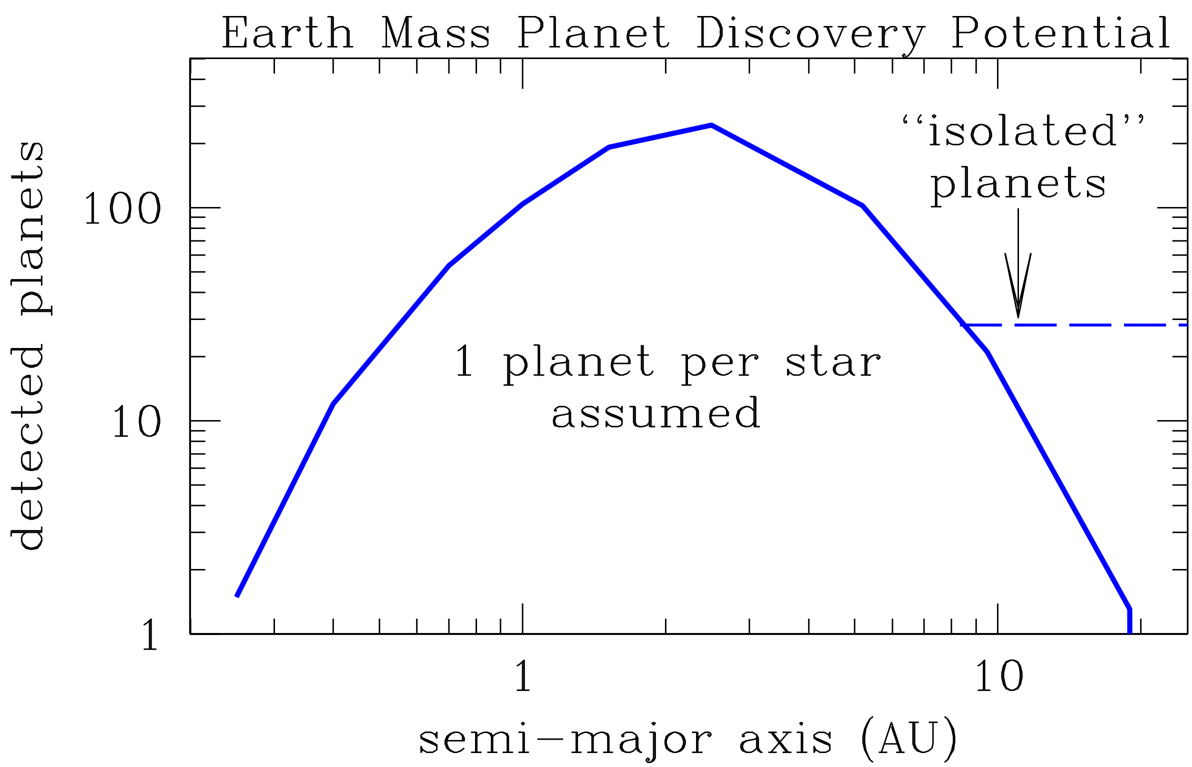

Fig. 8.— This is a plot of GEST's sensitivity to Earth-mass planets. The number of detected Earth-mass planets is shown as a function of the orbital semi-major axis assuming one such planet per lens star. At a semi-major axis of $\sim 10\,$AU, the number of planet detections reaches the lower limit of about 30 set by the free-floating planet detection calculation. Most of the planets detected with semi-major axis $\gg 10\,$AU will be detected in "isolation," without a detection of their host star.

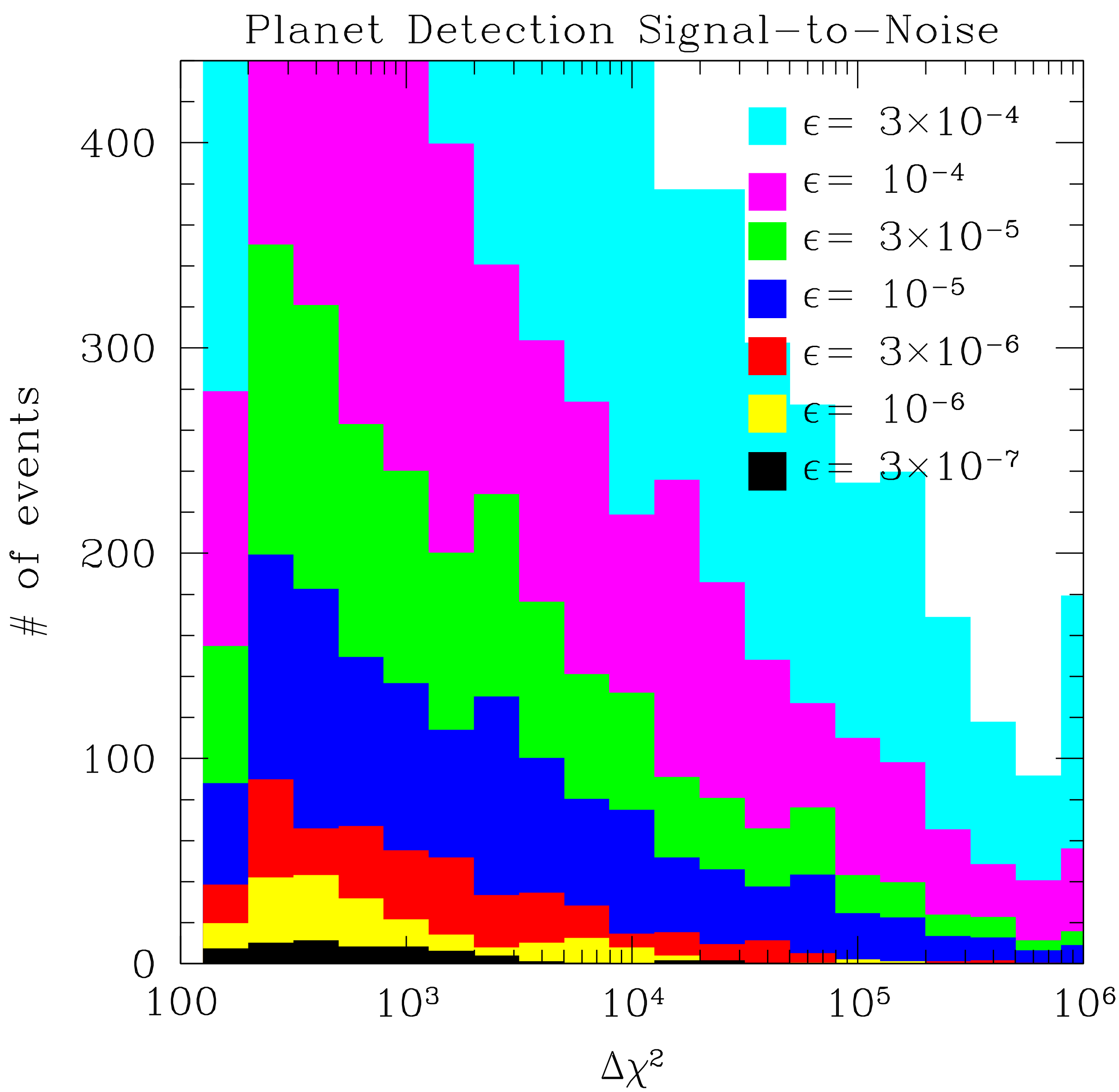

Fig. 9.— This is a histogram of the planetary detection significance, $\Delta\chi^2$, for different mass fractions, ϵ, ranging from $\epsilon = 3 \times 10^{-7}$ (the mass fraction of Mars) to $\epsilon = 3 \times 10^{-4}$ (the mass fraction of Saturn). For planets with an Earth-like mass fraction ($\epsilon = 3 \times 10^{-6}$) and above, more than half of the detected events have $\Delta\chi^2 > 800$ which corresponds to a 28σ detection.

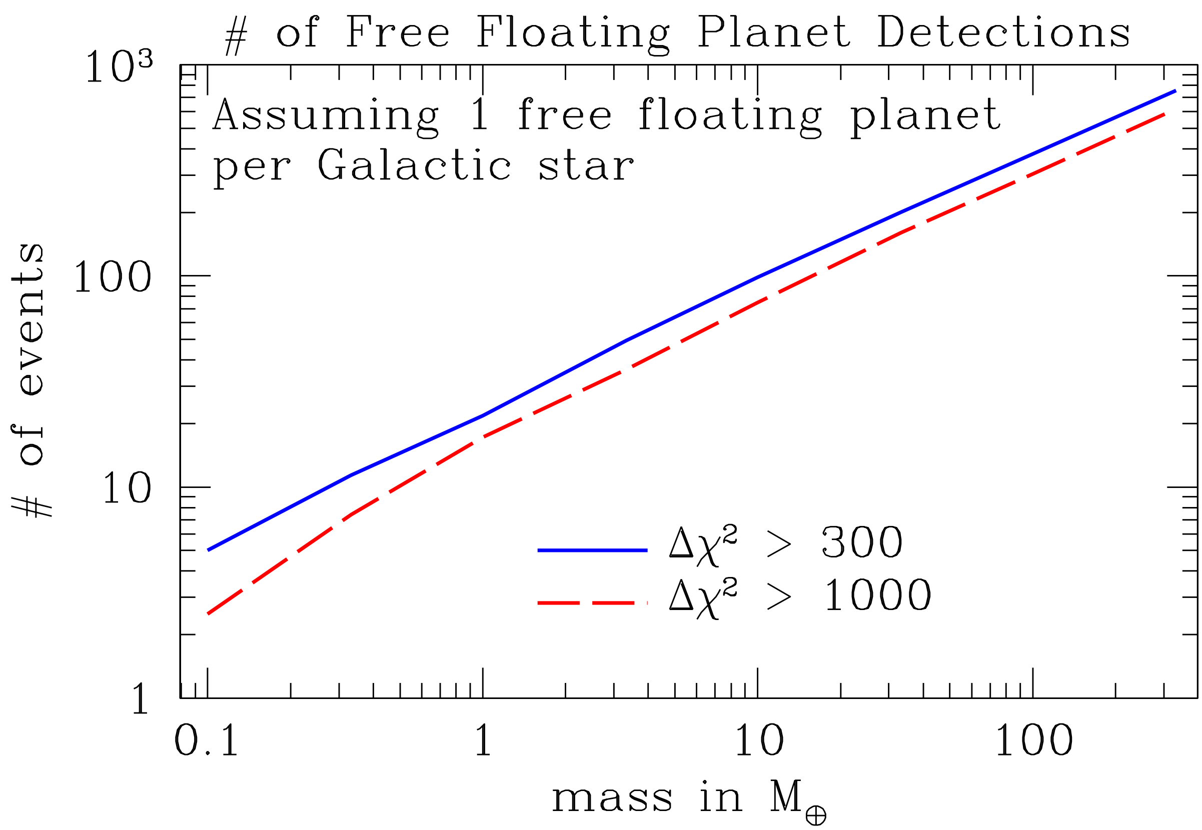

Fig. 10.— The number of free-floating planets to be discovered by GEST vs. planetary mass for 2 different detection criteria which are equivalent to 17σ and 30σ, respectively.

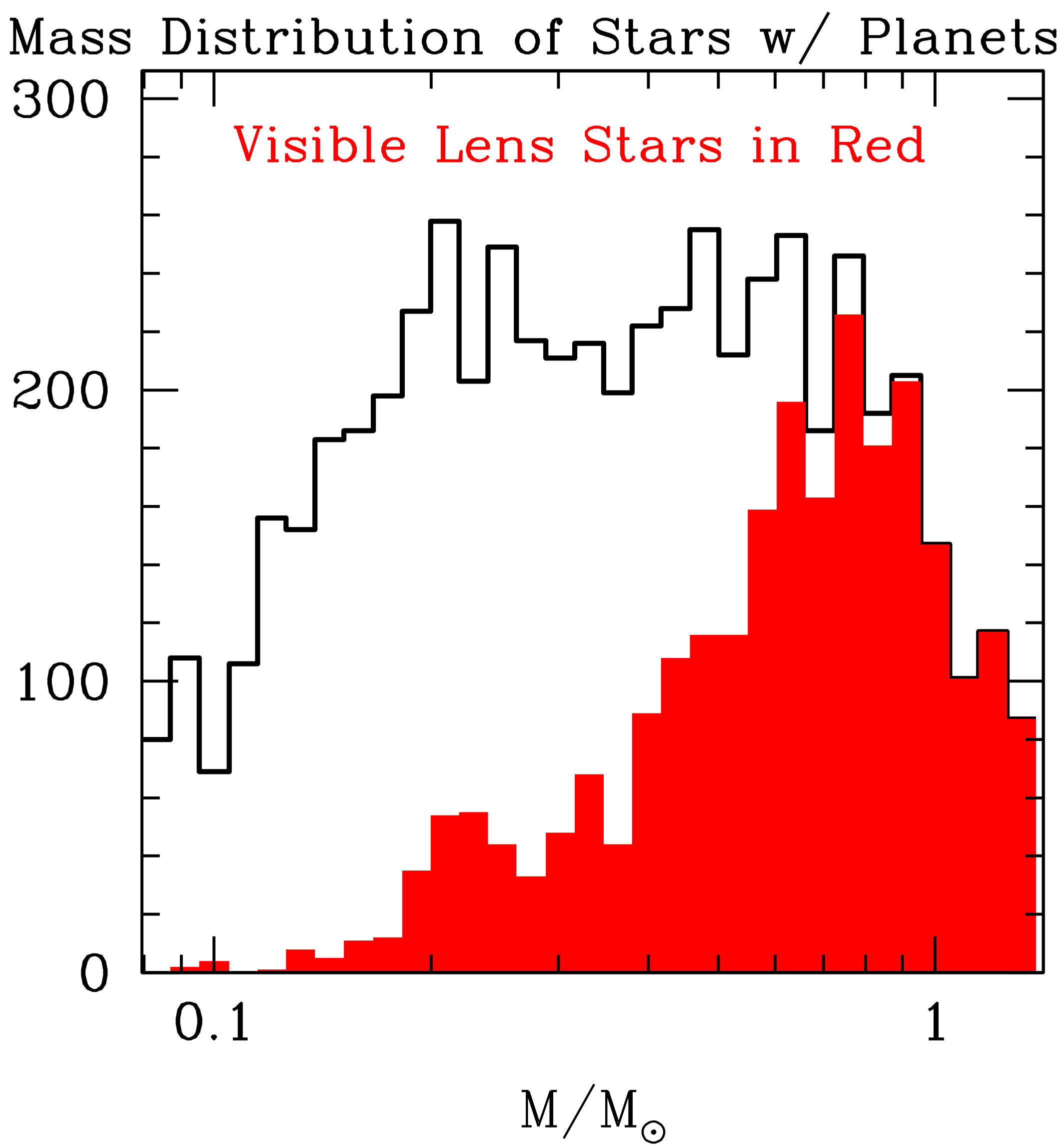

Fig. 11.— The simulated distribution of stellar masses is shown for stars with detected terrestrial planets. Lens stars are considered visible when they are at least 10% of the brightness of the source star, if they are not blended with a brighter star (besides the source). 1/3 of the events have visible lens stars.

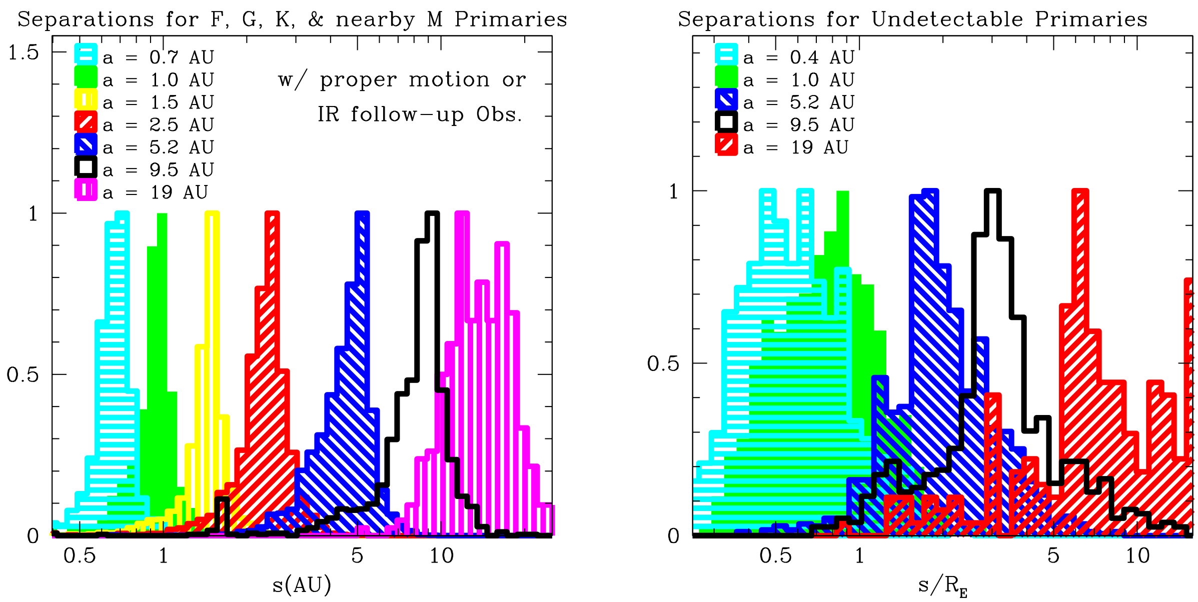

Fig. 12.— In the left panel, the measured separation for planets with different orbital semi-major axes is shown for the "visible" lens stars, for which the Einstein radius, R_E, can be determined . This allows the conversion of the measured separation, s, into physical units (AU). The following measurement accuracies are assumed: lens $I_{\rm lens}$: 20%, $I - K_{\rm lens}$: 10%, lens-source star centroids: 2 mas. The observed scatter in the measured separation relation is mostly due to the projection of the orbital plane on the sky. The distribution of measured star-planet separations is shown on the right for detected planets which orbit undetectable stars. The observed correlation between the planetary semi-major axis indicates that the measured separation can be used to estimate the semi-major axis with an accuracy of a factor of 2-3.

TABLE 1

TERRESTRIAL PLANET DETECTION SENSITIVITY FOR $\epsilon = 3 \times 10^{-6}$ AT 0.7-1.5 AU

ϵ	FOV (sq. deg.)	minimum error	FWHM	Effective Telescope Aperture (m) 1.0	**1.25**	1.6	2.0
3×10^{-6}	1.5	0.3%	0.32”	0.612	0.759	0.921	1.049
3×10^{-6}	2.0	0.3%	0.32”	0.726	0.908	1.058	1.251
3×10^{-6}	2.5	0.3%	0.32”	0.839	1.058	1.281	1.454
3×10^{-6}	1.5	0.15%	0.32”	0.652	0.813	1.006	1.167
3×10^{-6}	2.0	0.15%	0.32”	0.778	0.976	1.205	1.396
3×10^{-6}	2.5	0.15%	0.32”	0.905	1.138	1.405	1.625
3×10^{-6}	1.5	0.3%	0.24”	0.665	0.837	0.983	1.119
3×10^{-6}	**2.0**	**0.3%**	**0.24”**	0.795	**1.000**	1.179	1.336
3×10^{-6}	2.5	0.3%	0.24”	0.925	1.163	1.374	1.553
3×10^{-6}	1.5	0.15%	0.24”	0.704	0.889	1.071	1.251
3×10^{-6}	2.0	0.15%	0.24”	0.846	1.065	1.285	1.494
3×10^{-6}	2.5	0.15%	0.24”	0.988	1.241	1.499	1.737
3×10^{-6}	1.5	0.3%	0.16”	0.723	0.904	1.072	1.217
3×10^{-6}	2.0	0.3%	0.16”	0.865	1.079	1.278	1.448
3×10^{-6}	2.5	0.3%	0.16”	1.008	1.254	1.485	1.679
3×10^{-6}	1.5	0.15%	0.16”	0.763	0.956	1.152	1.331
3×10^{-6}	2.0	0.15%	0.16”	0.918	1.144	1.378	1.587
3×10^{-6}	2.5	0.15%	0.16”	1.073	1.332	1.604	1.844

This table shows the ratio of the number of terrestrial planet detections as a function of the telescope aperture, field-of-view (FOV), and effective point spread function FWHM. The parameters of the GEST MIDEX proposal are indicated in **bold**.

TABLE 2

TERRESTRIAL PLANET DETECTION SENSITIVITY FOR $epsilon = 10^{-5}$ AT 0.7-1.5 AU

ϵ	FOV (sq. deg.)	minimum error	FWHM	Effective Telescope Aperture (m)			
				1.0	**1.25**	1.6	2.0
10^{-5}	1.5	0.3%	0.32”	0.680	0.793	0.906	1.016
10^{-5}	2.0	0.3%	0.32”	0.803	0.937	1.074	1.202
10^{-5}	2.5	0.3%	0.32”	0.925	1.082	1.243	1.389
10^{-5}	1.5	0.15%	0.32”	0.709	0.834	0.974	1.114
10^{-5}	2.0	0.15%	0.32”	0.837	0.985	1.153	1.320
10^{-5}	2.5	0.15%	0.32”	0.965	1.136	1.322	1.526
10^{-5}	1.5	0.3%	0.24”	0.732	0.846	0.969	1.095
10^{-5}	**2.0**	**0.3%**	**0.24”**	0.863	**1.000**	1.148	1.296
10^{-5}	2.5	0.3%	0.24”	0.994	1.154	1.326	1.497
10^{-6}	1.5	0.15%	0.24”	0.758	0.885	1.034	1.190
10^{-5}	2.0	0.15%	0.24”	0.894	1.046	1.225	1.411
10^{-5}	2.5	0.15%	0.24”	1.031	1.207	1.415	1.632
10^{-5}	1.5	0.3%	0.16”	0.769	0.889	1.039	1.164
10^{-5}	2.0	0.3%	0.16”	0.906	1.049	1.230	1.372
10^{-5}	2.5	0.3%	0.16”	1.042	1.209	1.421	1.582
10^{-5}	1.5	0.15%	0.16”	0.794	0.928	1.101	1.256
10^{-5}	2.0	0.15%	0.16”	0.936	1.094	1.302	1.483
10^{-5}	2.5	0.15%	0.16”	1.078	1.261	1.504	1.712

This table shows the ratio of the number of terrestrial planet detections as a function of the telescope aperture, field-of-view (FOV) and effective point spread function FWHM. The parameters of the GEST MIDEX proposal are indicated in **bold**.

TABLE 3
PLANETARY TRANSITS FROM GEST

Semi-major axis (AU)	Period (yrs.)	# of detections	transits per planet	transit duration
0.04	~ 0.01	5,000,000	~ 200	1.6
0.4	~ 0.3	600,000	~ 7	5
1.0	~ 1.3	160,000	~ 2	8
2.0	~ 3.7	40,000	1	11
5.2	~ 15	6,000	1	18
9.5	~ 40	1,300	1	24
19.5	~ 110	200	1	35

This table shows the number of expected transit planet detections for planets with a radius at least as large as that of Saturn for a three year GEST mission assuming 8 months of observations per year. The planet detection numbers assume 1 planet per star.